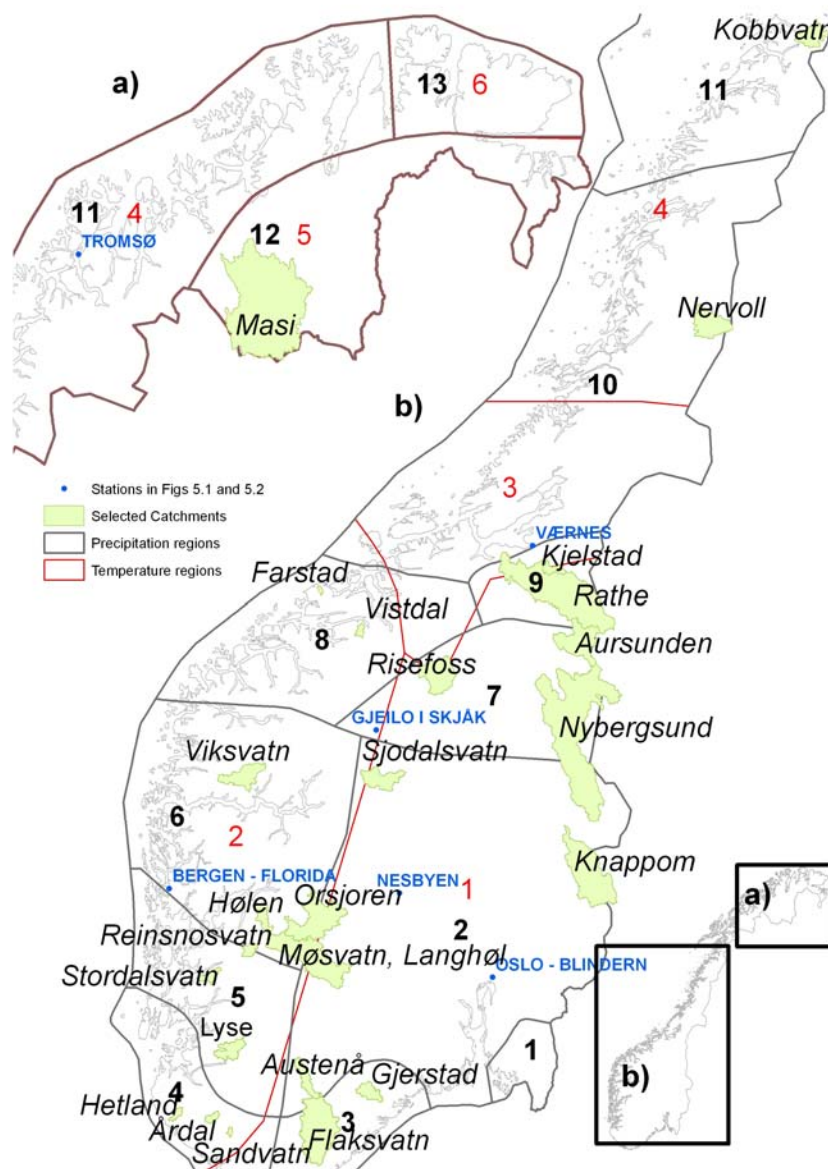


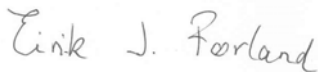


Empirically downscaled precipitation and temperature up to year 2050 for twenty-five Norwegian catchments

Torill Engen-Skaugen, Rasmus Benestad and Eirik J. Førland



Title Empirically downscaled precipitation and temperature up to year 2050 for twenty-five Norwegian catchments	Date 08.12.2008
Section Climate	Report no. no. 23 a/08
Author(s) Torill Engen-Skaugen, Rasmus Benestad and Eirik J. Førland	Classification <input checked="" type="checkbox"/> Free <input type="checkbox"/> Restricted
	ISSN 1503-8025
	e-ISSN 1503-8025
Client(s) EBL Norwegian Electricity Industry Association	Client's reference MKU-1.8_06
Abstract Area averaged temperature and precipitation were downscaled for 25 different Norwegian catchments for the period 1960-2050, based on a multi-model ensemble of the most recent global climate models. The results point to a future warming at all catchments but the projected trends for the precipitation gave a more mixed picture, depending on season and location. A substantial spread within the multi-model ensemble illustrates the large degree of uncertainty associated with such simulations and analysis.	
Keywords Climate change, Empirical statistical downscaling (ESD), temperature, precipitation	

Disciplinary signature  <hr/> Inger Hanssen-Bauer	Responsible signature  <hr/> Eirik J. Førland
--	---

Postal address	Office	Telephone	Telefax	e-mail: met@met.no	Bank account	Swift code
P.O.Box 43, Blindern NO-0313 OSLO Norway	Niels Henrik Abelsvei 40	+47 22 96 30 00	+47 22 96 30 50	Internet: met.no	7694 05 00628	DNBANOKK

1 Introduction

Levels of atmospheric concentrations of long-lived green house gases, such as CO₂, have risen since the industrial revolution and this increase lead to global surface warming (IPCC, 1995; Houghton et al., 2001; Solomon et al., 2007). Most recent estimates suggest that the global mean surface temperature on Earth has increased by 0.74 ± 0.18 °C over the last 100 years (Solomon et al., 2007). Further increase in levels of greenhouse gases will warm the surface further (Meehl et al., 2007; Christensen et al., 2007).

The aim of the present study is to estimate the local changes in precipitation and temperature associated with global warming. It should be noted that there are uncertainties with the CMIP3 simulations, on which the present results are based, as the GCMs from the CMIP3 are not initialised by taking into account the present state of the atmosphere and oceans (do not involve so-called 'data assimilation'), and may not capture the right phase of regional decadal cycles (such as the Atlantic Meridian Overturning/Thermohaline Circulation). On the other hand, the CMIP3 is believed to provide a more reliable picture on a longer time horizon when changes in the forcings (boundary conditions) become more important than the starting point (initial conditions). Hence, this caveat should be kept in mind when using these results and it is really the long-term trends which are more reliable. The results presented here will contain the early part of these long-term trends.

Part of the problems is due to incomplete understanding of the climate system. The important mechanisms causing variability such as El Niño Southern Oscillation (ENSO) and the North Atlantic Oscillation (NAO) for instance are probably still not completely understood (Sarachik et al., 1996; Anderson and Carrington, 1994; Philander, 1989; Christensen et al., 2007). Due to discretisation and gridding of data, it is unlikely that the global GCMs will simulate regional details realistically (Crane and Hewitson, 1998; Zorita and von Storch, 1997; von Storch et al., 1993b; Robinson and Finkelstein, 1991). However, a wide range of GCMs predict observed regional features (e.g. the NAO, ENSO, the Hadley Cell, atmospheric jets), thus it is believed that the GCMs may be useful for predicting large scale features. Global climate models tend to have a coarse spatial resolution, and are unable to represent aspects with spatial scales smaller than the grid box size. The global climate models are also unable to account for details in the climate statistics within a small region, such as local temperature gradients.

Projections for temperature and precipitation for the near future (up to 2050) are here made for twenty-five selected catchments in Norway, and the work has been funded by the Norwegian Electricity Industry Association (EBL). Runoff from the twenty-five selected catchments are analysed in Engen-Skaugen et al. (2007). The downscaling method used is Empirical Statistical Downscaling (ESD). ESD methods are less computer demanding than dynamical downscaling methods, and are easily carried out given sufficient data. Requirements for the method are historic time-series of temperature and precipitation representative for the twenty-five catchments and availability of GCM runs and ERA40 data (See Section 3.2). The method has been used in several previous studies and is therefore well-documented (Benestad, 2004; Benestad, 2005; Benestad et al. 2007; Engen-Skaugen et al., 2007; Benestad 2008 a,b,c; Benestad et al., 2008).

It is important to keep in mind possible limitations of statistical downscaling, especially when applied to model results from greenhouse (GHG) integrations. The statistical models are based on historical data, and there is no guarantee that the past statistical relationships between different data fields will hold in the future. However, tests made over the past suggest that the relationship between the large scales and the local scales do not change as long as appropriate predictors are chosen. This aspect is discussed further in Benestad et al., (2008). Dynamical downscaling also involves some limitations, and the statistical and dynamical downscaling approaches have different strengths and weaknesses (Benestad, 2007). One should also be concerned about the uncertainties associated with the GCM results as well as those of the downscaling methods themselves (Wilby et al., 1998). It is well known that low resolution GCMs are far from perfect, and that they have problems associated with for instance cloud representation, atmosphere-ocean coupling, and artificial climate drift (Bengtsson, 1996; Anderson and Carrington, 1994; Treut, 1994; Christensen et al., 2007).

The description of the selected catchments is given in Section 2. Analyses of runoff from the catchments are reported in Engen-Skaugen et al. (2007). Daily precipitation sums and mean daily temperature within twenty-five selected catchments are based on grids with daily time resolution and spatial resolution of 1 x 1 km² (Section 3.1). The grids are interpolated from daily values of temperature and precipitation estimated from observations. These time series represent the selected catchments and are used as observations when establishing ESD models for temperature and precipitation projections. The ERA40 re-analysis is documented in Section 3.2. The scenarios follow the SRES emission scenario A1b (IPCC, 2000). The ESD-analyses was based on the most recent global climate model (GCM) simulations (34 and 38 GCMs for precipitation and temperature respectively) reported in IPCC AR4 (Meehl et al., 2007) (Section 3.3). The present study is based on 14 different GCMs following the SRES emission scenario A1b. The number of simulations for the different climatic variable and time interval is shown in Appendix A, however, not all of these GCM results were used; a quality check was implemented that weeded out poorly performing models. More details are given in the ESD - method description (Section 4).

Two annex reports are produced showing the results for each catchment for precipitation (Engen-Skaugen et al., 2008a) and temperature (Engen-Skaugen et al., 2008b). These are referred to in section 5. Discussion of the results with concluding remarks are given in Section 6.

2 Description of the selected catchments

A selection of twenty-five catchments is chosen in accordance with the regions of interests of members of the Norwegian Electricity Industry Association (EBL) (Figure 2.1). The catchments represent different landscape types, including mountains and alpine terrain, subalpine and boreal forests, non-forested areas below the tree line, lakes, bogs and glaciers. The catchments areas range from 23 to 5693 km², cover elevations between 8 and 2345 m a.s.l. each of which holding different characteristics (e.g. coastal or inland regions, high mountain or low land area, terrain gradient, precipitation amounts, seasonal temperature variations). Characteristics of the catchments are given in Table 2.1, and hypsographic curve based on digital terrain model (DTM) for all catchments are presented in the Figures 2.2-2.7. The spatial resolution of the DTMs is 1 x 1 km² (DTM1km) or 100 x 100 m² (DTM100m). The DTM100m is used for small catchments and catchments at the Swedish boarder. The DTM1km cover only the Norwegian main land. Maximum elevation of the catchments (Table 2.1) is obtained from the digital height point database (N50, Source © Norge digitalt), it may therefore not coincide with the highest elevation of the hypsographic curves.

Regions with fairly homogeneous concerning temperature (6 regions) and precipitation (13 regions) variations in Norway are defined by Hanssen-Bauer and Nordli (1998) and Hanssen-Bauer and Førland (1998) respectively. The homogeneous temperature and precipitation regions are shown in Figure 2.1. Temperature and precipitation projections for the future for the homogeneous regions are established in Benestad (2008a).

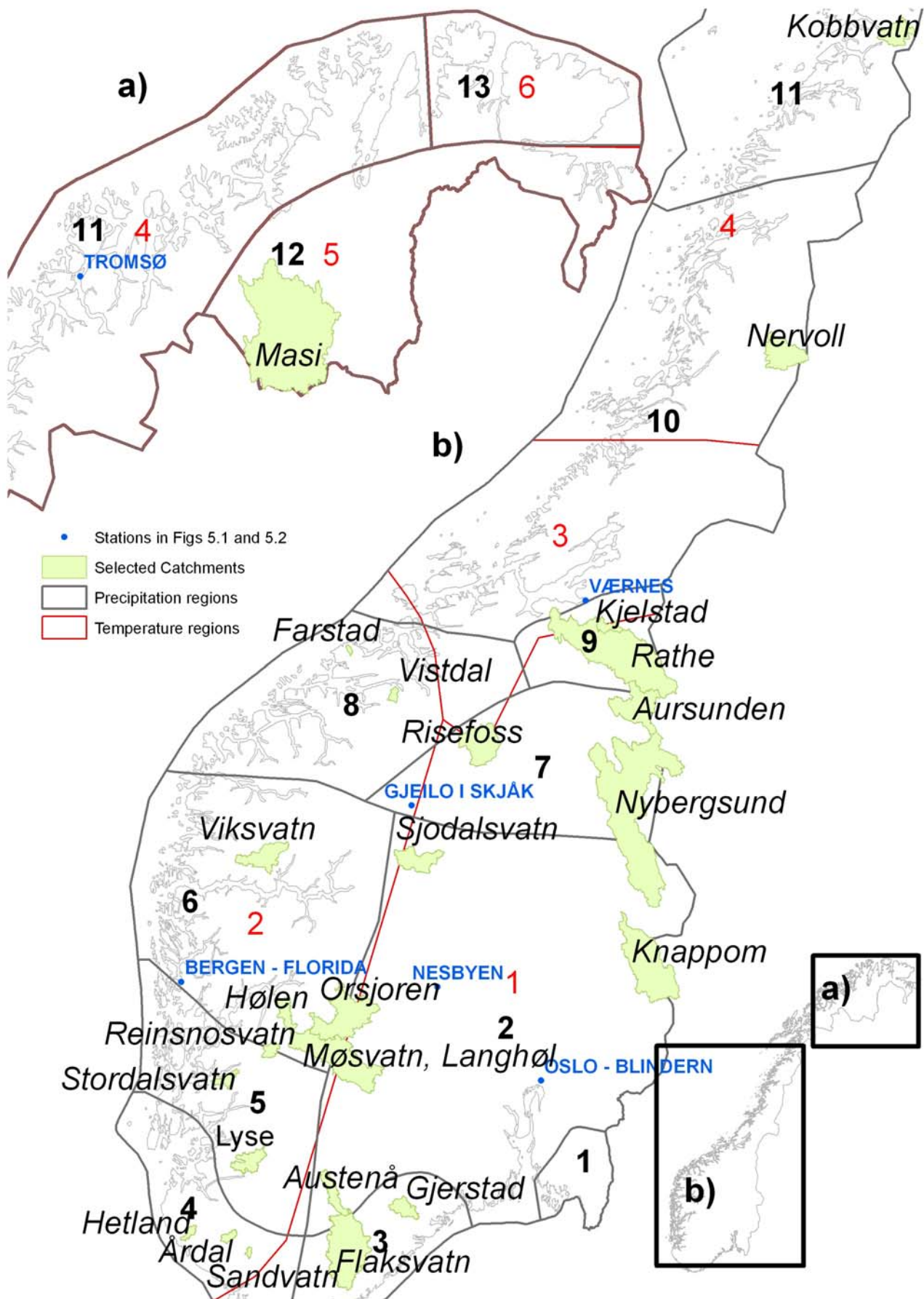


Figure 2.1 Location of the 25 selected catchments. Temperature and precipitation regions, defined by fairly homogeneous variations, are shown in the figure.

Hypsographic curves

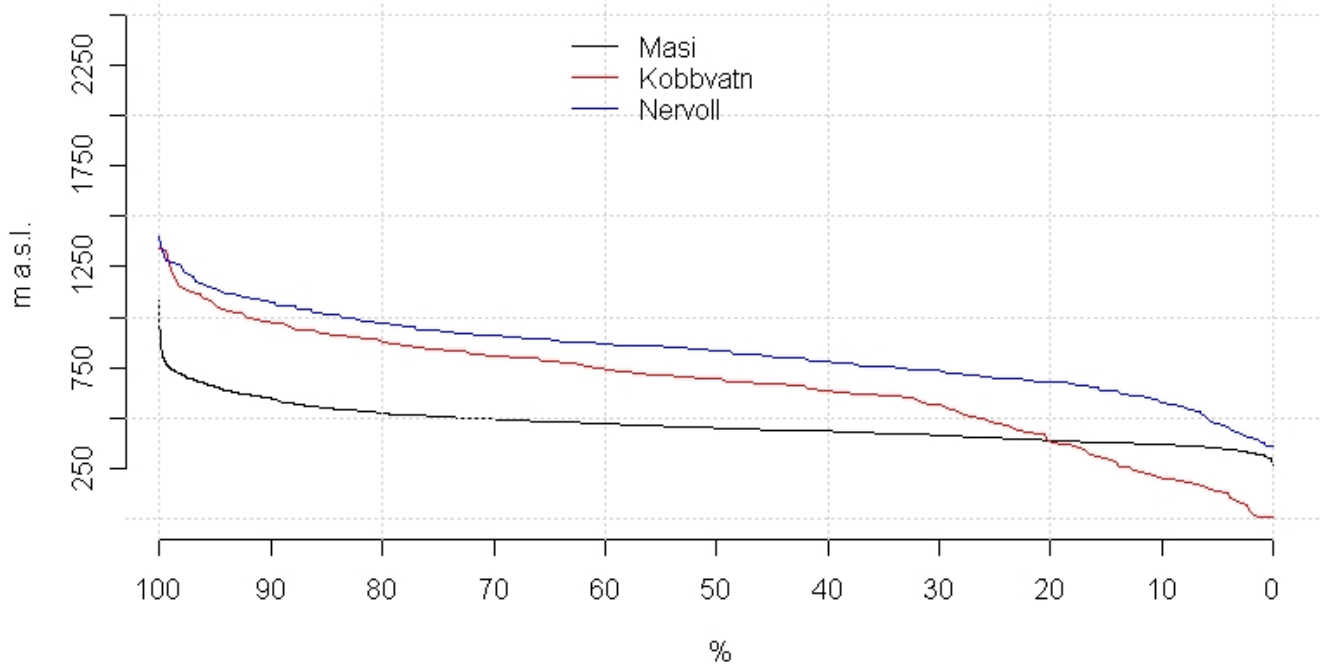


Figure 2.2 Hypsographic curves of the catchments Masi, Kobbvatn and Nervoll. The curve is established from DTM1km (Kobbvatn, Nervoll) and DTM100m (Masi) resolution.

Hypsographic curves

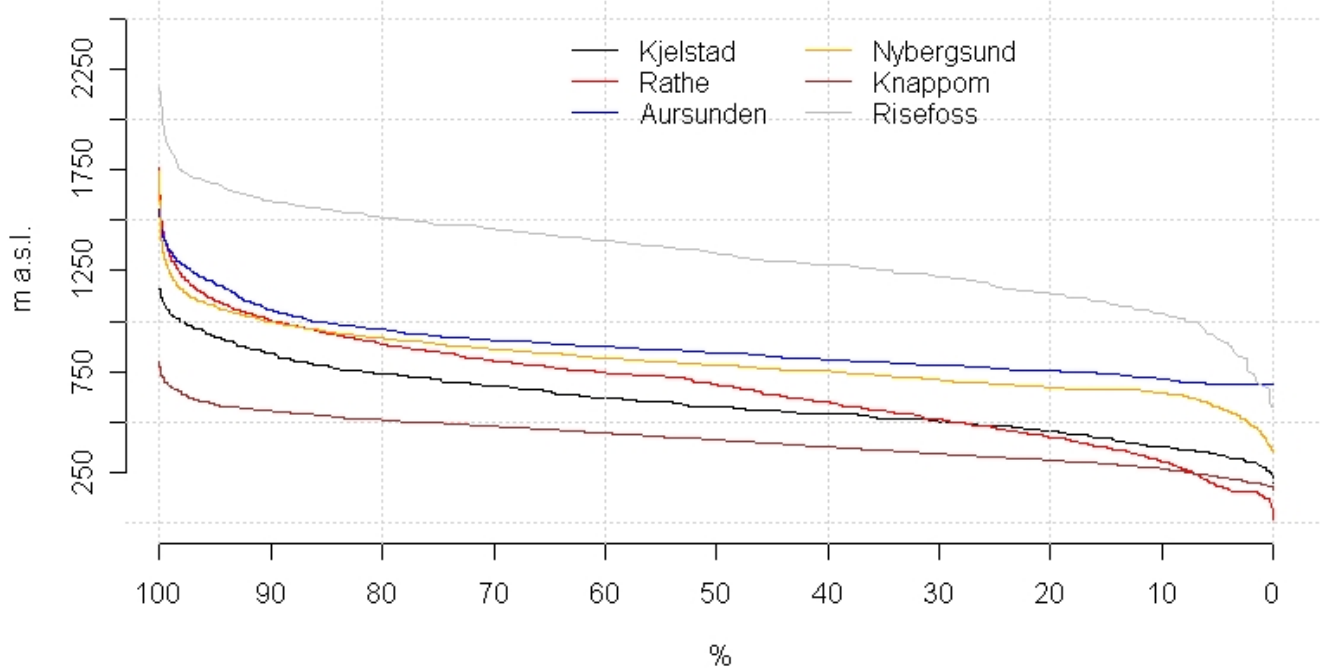


Figure 2.3 Hypsographic curves of the catchments Kjelstad, Rathe, Aursunden, Nybergsund, Knappom and Risefoss. The curve is established from DTM1km (Risefoss) and DTM100m (Kjelstad, Rathe, Aursunden, Nybergsund, Knappom) resolution.

Hypsographic curves

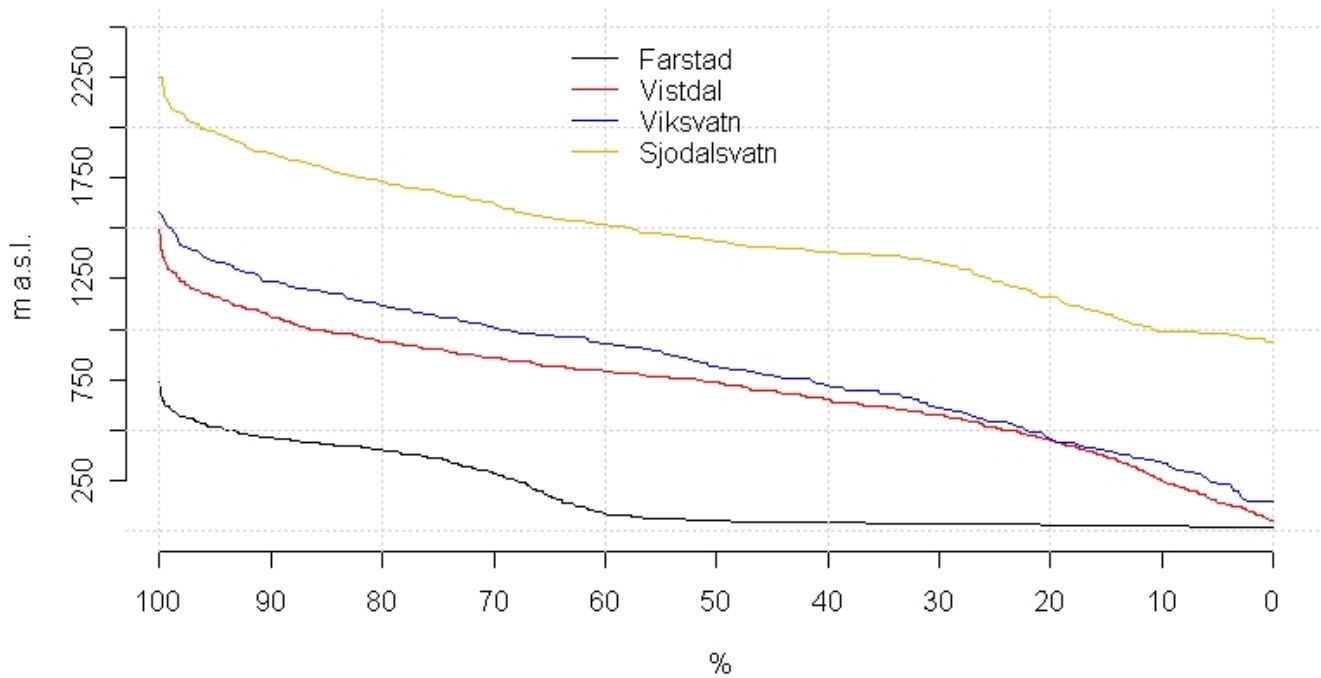


Figure 2.4 Hypsographic curves of the catchments Farstad, Vistdal, Viksvatn and Sjordalsvatn. The curve is established from DTM1km (Viksvatn, Sjordalsvatn) and DTM100m (Farstad, Vistdal) resolution.

Hypsographic curves

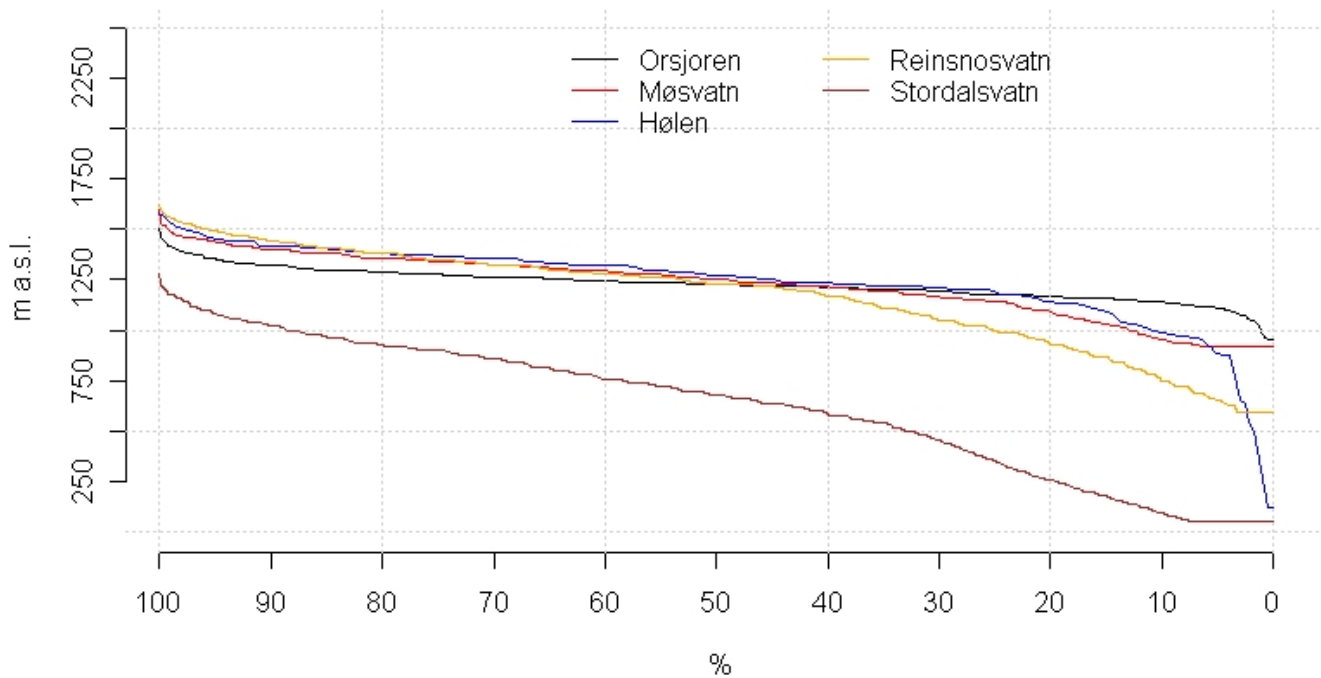


Figure 2.5 Hypsographic curves of the catchments Orsjoren, Møsvatn, Hølen, Reinsnosvatn and Stordalsvatn. The curve is established from DTM1km (Orsjoren, Møsvatn, Hølen) and DTM100m (Reinsnosvatn, Stordalsvatn) resolution.

Hypsographic curves

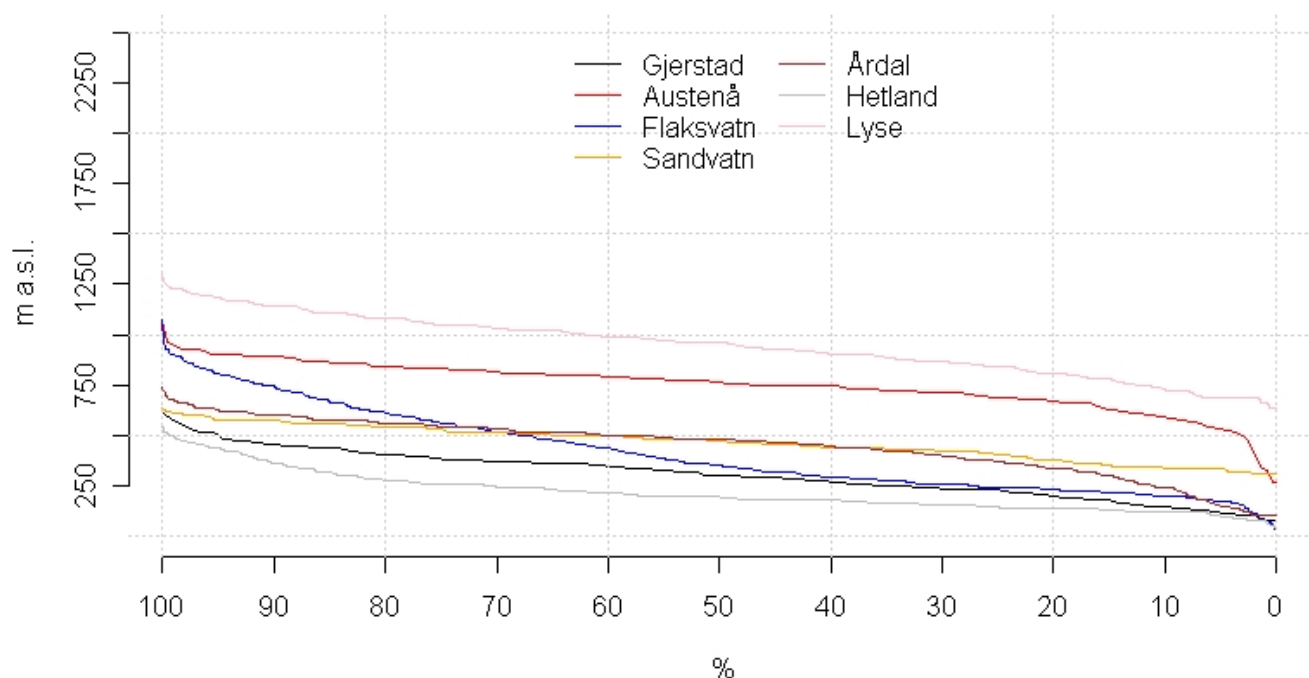


Figure 2.6 Hypsographic curves of the catchments Gjerstad, Austenå, Flaksvatn, Sandvatn, Årdal, Hetland and Lyse. The curve is established from DTM1km (Gjerstad, Austenå, Flaksvatn, Hetland, Lyse) and DTM100m (Sandvatn Årdal) resolution.

Table 2.1 Meta information of the twenty-five selected catchments. Max, min and mean values of the terrain is from 1x1 km 2 terrain grid model covering the Norwegian mainland.

* temperature and precipitation estimate represents only the Norwegian part of the catchment

Catchment No.	Catchment name	AREA L [KM ²]	Precipitation (61-90) [mm/year]	Mean annual temperature [°C]	Mean elevation [m a.s.l.]	Minimum elevation [m a.s.l.]	Max. elevation [m a.s.l.]
212.1	Masi	5626.3	479	-3.2	463.9	265	1086
167.3	Kobbvatn	389	2537	0.1	665.5	8	1517
151.15	Nervoll	652.9	1542*	-1.6	826.9	360	1699
123.31	Kjelstad	142.2	1430	2.1	602.9	280	1171
123.2	Rathe	3052.8	1292*	1.6	630.2	44	1762
2.113	Aursunden	849	987*	-0.6	853.3	690	1525
311.6	Nybergsund	4420.2	863*	-0.7	794.6	355	1755
2.142	Knappom	1649.8	769*	1.7	410.3	180	809
109.9	Risefoss	743.6	1035	-1.9	1328.6	580	2286
107.3	Farstad	23.45	2476	5.2	148.6	19	667
104.23	Vistdal	66.4	2666	2.8	703.1	60	1552

Catchment No.	Catchment name	Area [km ²]	Precipitation (61-90) [mm/year]	Mean annual temperature [°C]	Mean elevation [m a.s.l.]	Minimum elevation [m a.s.l.]	Max. elevation [m a.s.l.]
83.2	Viksvatn	506.6	3786	2.2	810.9	146	1636
2.13	Sjodalsvatn	480	1278	4.3	1458.9	940	2345
15.79	Orsjoren	1177.4	1504	-2.1	1228.4	954	1540
16.19	Møsvatn, Langhøl	1509.7	1638	-1.5	1227.2	919	1630
50.1	Hølen	232.5	2623	0.3	1244.1	120	1690
48.5	Reinsnosvatn	120.8	3117	0.8	1162.8	597	1606
41.1	Stordalsvatn	129.5	4254	3.7	647.2	51	1250
18.1	Gjerstad	236.7	1373	4.7	309.6	80	659
20.2	Austenå	276.7	1786	2.4	753.5	270	1072
20.3	Flaksvatn	1777	1659	4.4	353.9	35	1072
26.21	Sandvatn	27.5	2621	4.7	402	320	630
26.2	Årdal	77.3	3126	4.7	438.3	107	740
27.26	Hetland	69.5	2346	6.1	219.7	60	532
257.257	Lyse	317.1	4353	1.8	946.9	506	1304

3 Data

3.1 Precipitation and temperature representing catchments

Temperature and precipitation is measured at stations which register the very local values that in essence can be considered as point-measurement. Thus, the temperature and precipitation values measured in one or several points within a catchment may not be representative for an area or catchments, especially for large catchments with complex terrain. Daily precipitation sum and mean daily temperature are therefore interpolated to daily grids with spatial resolution of 1 x 1 km² over the Norwegian mainland (Tveito et al., 2005; Jansson, et al., 2007). The daily 1 x 1 km² grids contain uncertainties due low density of the available temperature and precipitation stations as well as the fact that the local measurement may not be representative of the 1km² area. In Norway the density of temperature and precipitation stations increased from the beginning of measurements (before 1900) until ~1970. The number of stations was stable within the twenty-year period 1970-1990, but it has decreased after 1990. The uncertainty of the estimates follows the number of stations (Tveito, 2007) (Fig. 3.1). Another aspect is that most of the stations are situated in low lying regions (Fig. 3.2). High-elevation regions with complex terrain are therefore associated with larger uncertainty.

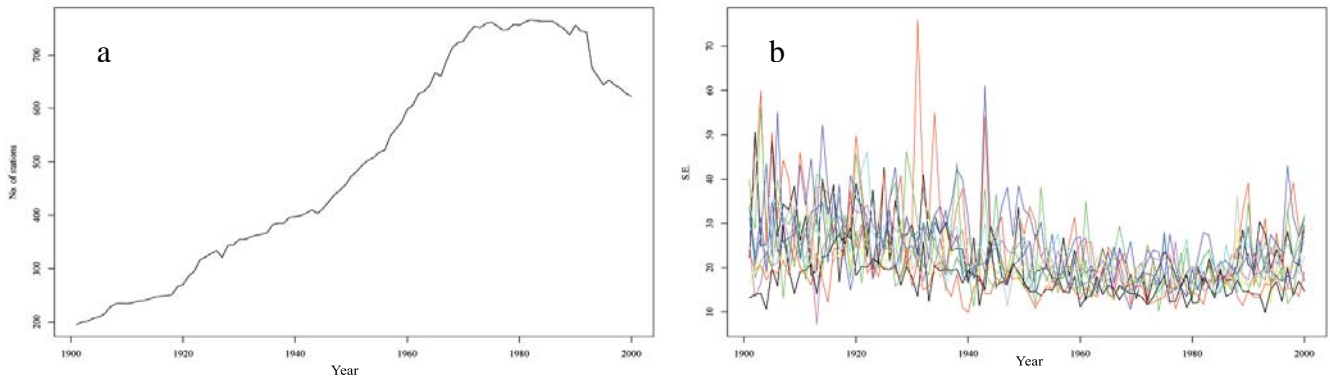


Figure 3.1. a) Number of temperature stations available from the Norwegian meteorological institute from 1900 to present. b) Standard deviation of the gridded temperature estimates indicating the uncertainty of the grids. The lower the number of stations, the larger uncertainty associated with the temperature estimates (page 133 and 134 in Tveito et al., 2008)

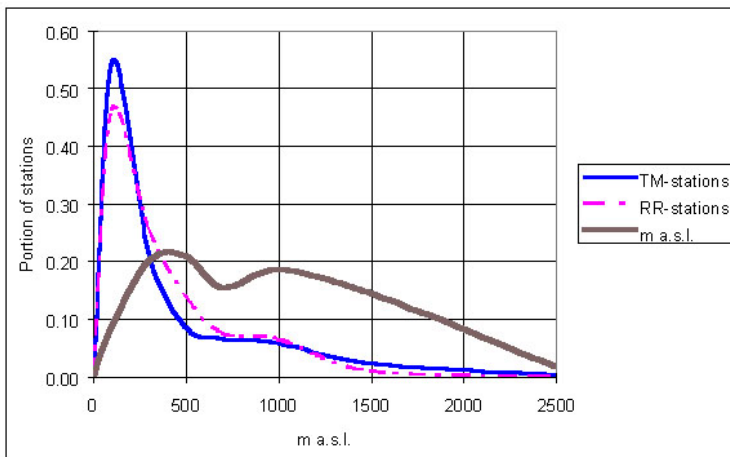


Figure 3.2. The portion of temperature (TM) and precipitation (RR) stations compared to altitude (From Tveito et al., 2005)

The interpolation method used is triangulation on temperature (Jansson et al., 2007; Tveito et al., 2005) and precipitation. Triangulation of daily precipitation values are used with corrections for elevation and under catch of precipitation. Daily grids are derived for the period 1961-present, and an evaluation of the gridded results is given in Jansson et al. (2007). Precipitation representing a catchment is computed here by averaging the values in the grid-cells within the catchment.

Mean monthly temperature and precipitation sums (for the normal period 1961-1990) are presented in figure 3.3-3.27 for the twenty-five catchments, all based on the gridded dataset. The mean annual precipitation within the same period for all the selected catchments is also listed in Table 2.1.

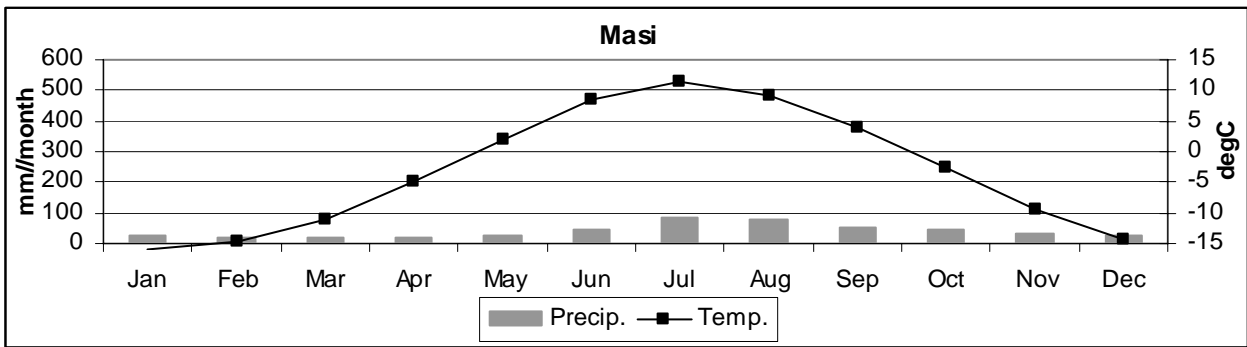


Figure 3.3 Mean monthly temperature and precipitation sum representing Masi catchment. The estimates are obtained from interpolation of daily mean values estimated from observations.

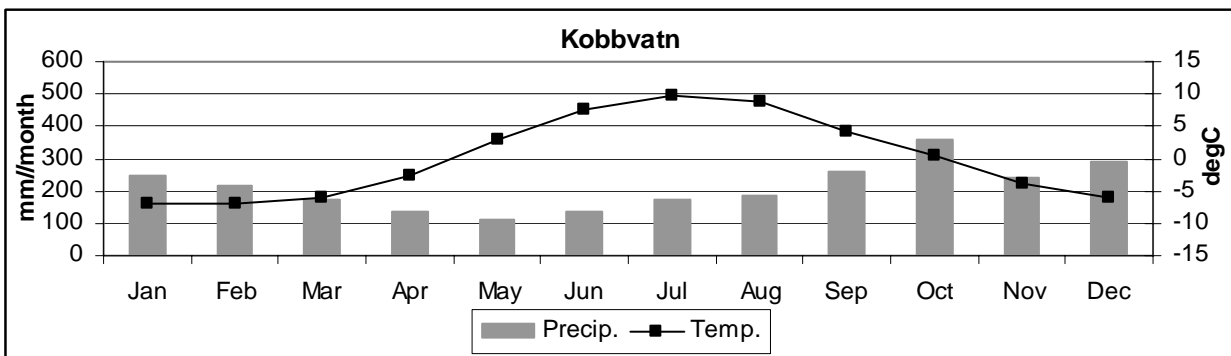


Figure 3.4 Mean monthly temperature and precipitation sum representing Kobbvatn catchment. The estimates are obtained from interpolation of daily mean values estimated from observations.

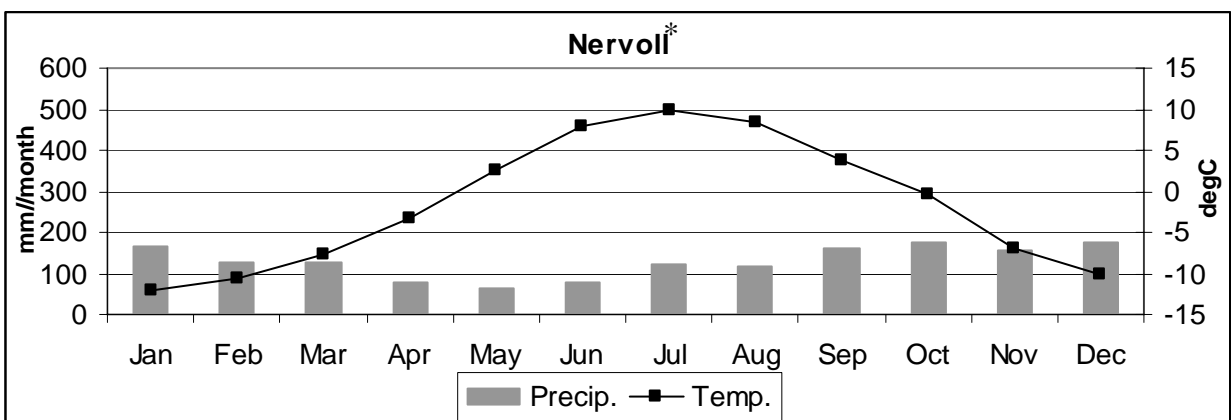


Figure 3.5 Mean monthly temperature and precipitation sum representing Nervoll catchment. The estimates are obtained from interpolation of daily mean values estimated from observations.

* temperature and precipitation estimate represents only the Norwegian part of the catchment

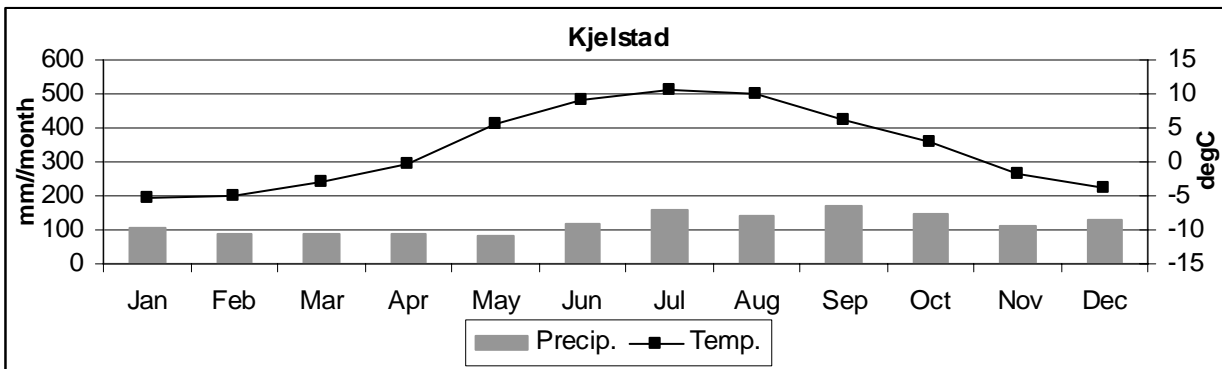


Figure 3.6 Mean monthly temperature and precipitation sum representing Kjelstad catchment. The estimates are obtained from interpolation of daily mean values estimated from observations.

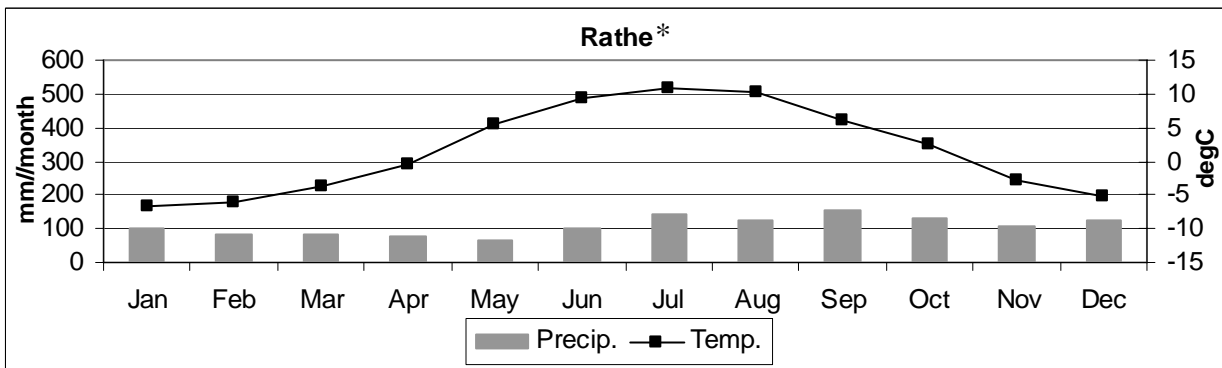


Figure 3.7 Mean monthly temperature and precipitation sum representing Rathe catchment. The estimates are obtained from interpolation of daily mean values estimated from observations.

* temperature and precipitation estimate represents only the Norwegian part of the catchment

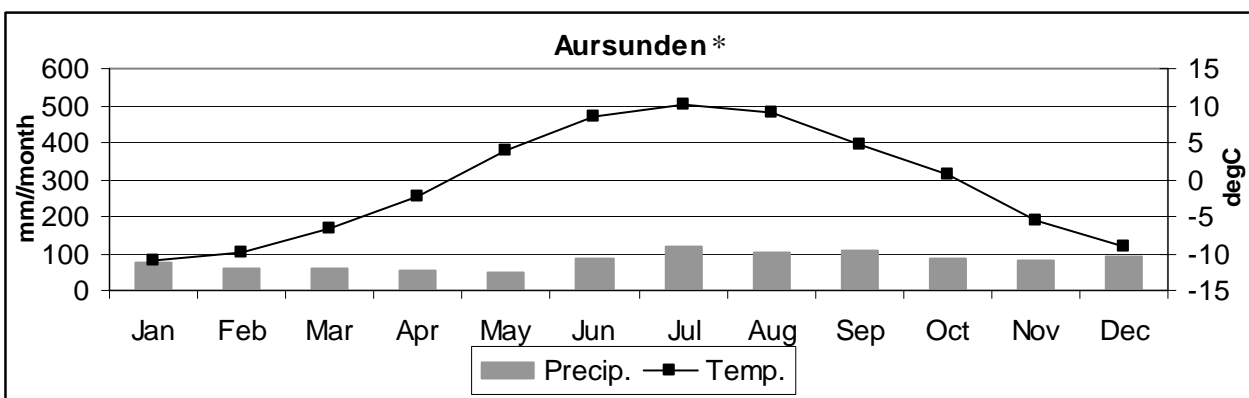


Figure 3.8 Mean monthly temperature and precipitation sum representing Aursunden catchment. The estimates are obtained from interpolation of daily mean values estimated from observations.

* temperature and precipitation estimate represents only the Norwegian part of the catchment

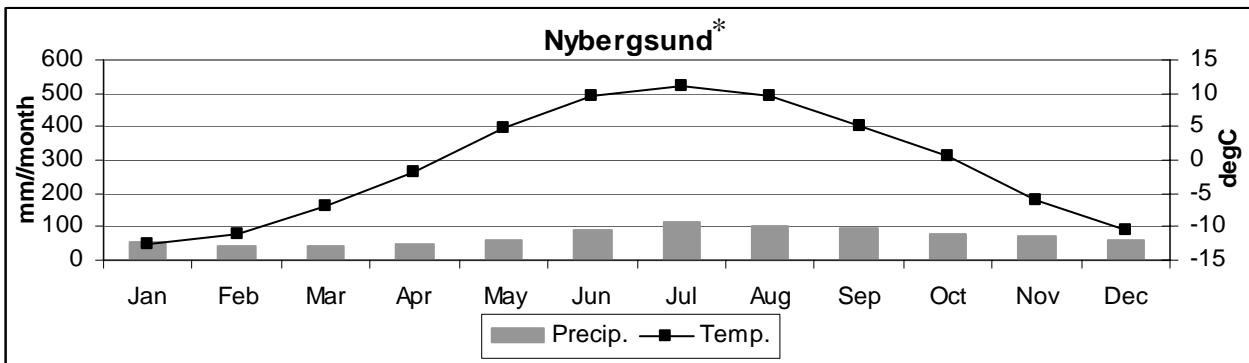


Figure 3.9 Mean monthly temperature and precipitation sum representing Nybergsund catchment. The estimates are obtained from interpolation of daily mean values estimated from observations.
 * temperature and precipitation estimate represents only the Norwegian part of the catchment.

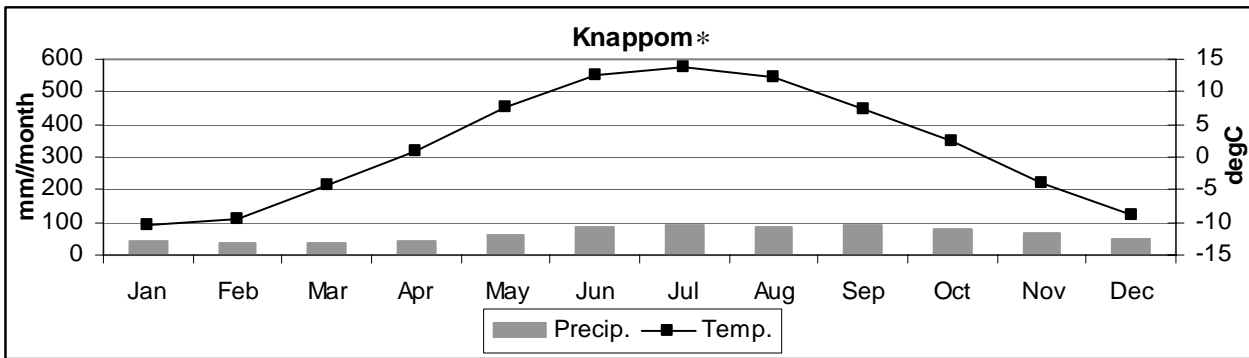


Figure 3.10 Mean monthly temperature and precipitation sum representing Knappom catchment. The estimates are obtained from interpolation of daily mean values estimated from observations.
 * temperature and precipitation estimate represents only the Norwegian part of the catchment

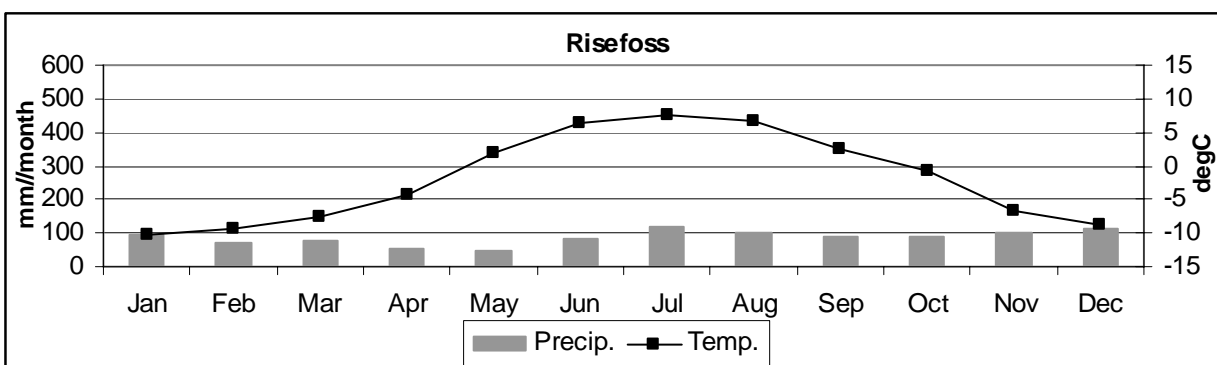


Figure 3.11 Mean monthly temperature and precipitation sum representing Risefoss catchment. The estimates are obtained from interpolation of daily mean values estimated from observations.

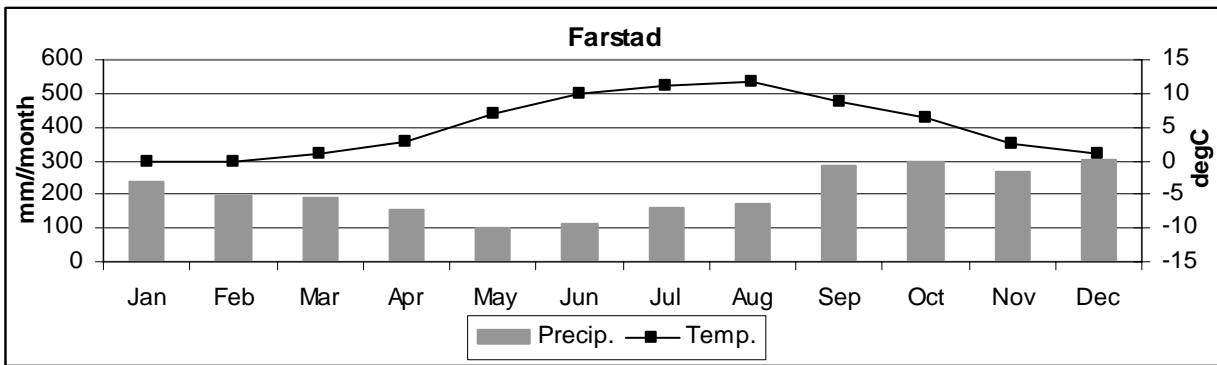


Figure 3.12 Mean monthly temperature and precipitation sum representing Farstad catchment. The estimates are obtained from interpolation of daily mean values estimated from observations.

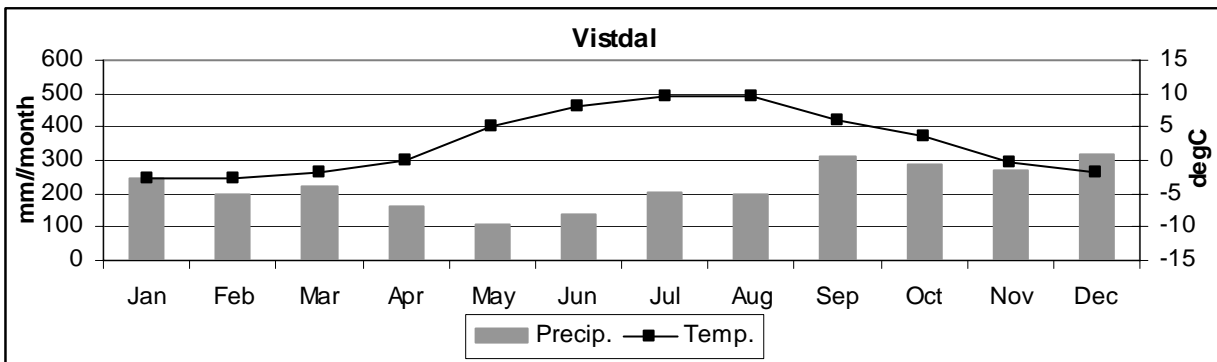


Figure 3.13 Mean monthly temperature and precipitation sum representing Vistdal catchment. The estimates are obtained from interpolation of daily mean values estimated from observations.

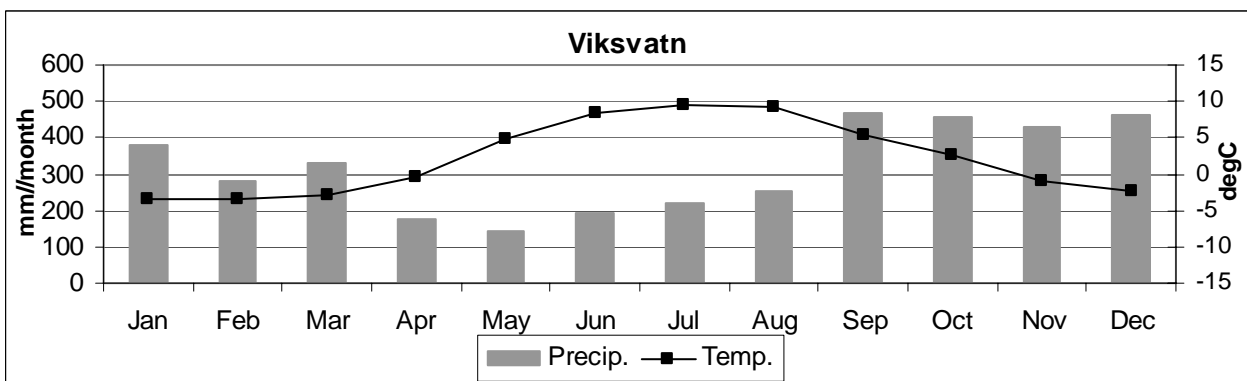


Figure 3.14 Mean monthly temperature and precipitation sum representing Viksvatn catchment. The estimates are obtained from interpolation of daily mean values estimated from observations.

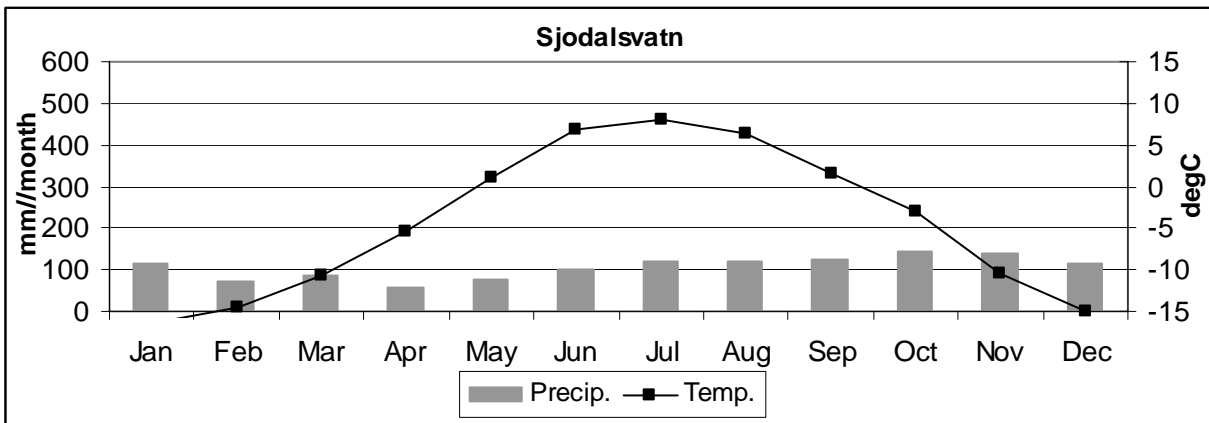


Figure 3.15 Mean monthly temperature and precipitation sum representing Sjordalsvatn catchment. The estimates are obtained from interpolation of daily mean values estimated from observations.

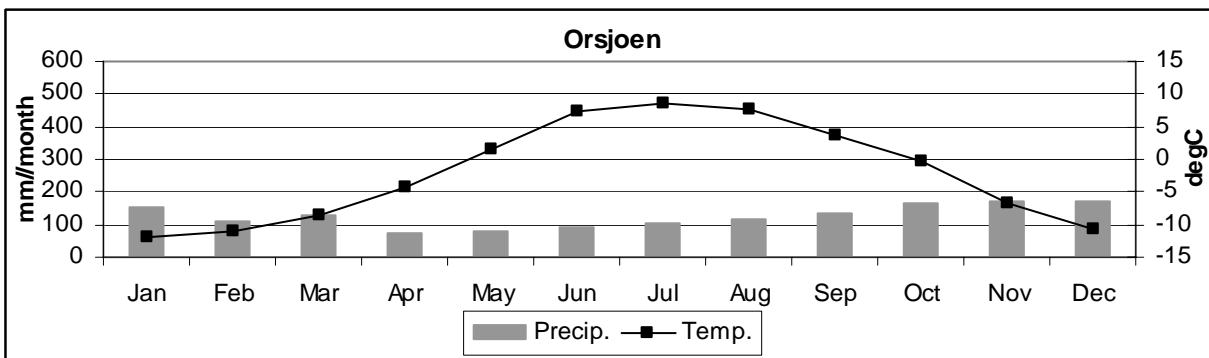


Figure 3.16 Mean monthly temperature and precipitation sum representing Orsjoen catchment. The estimates are obtained from interpolation of daily mean values estimated from observations.

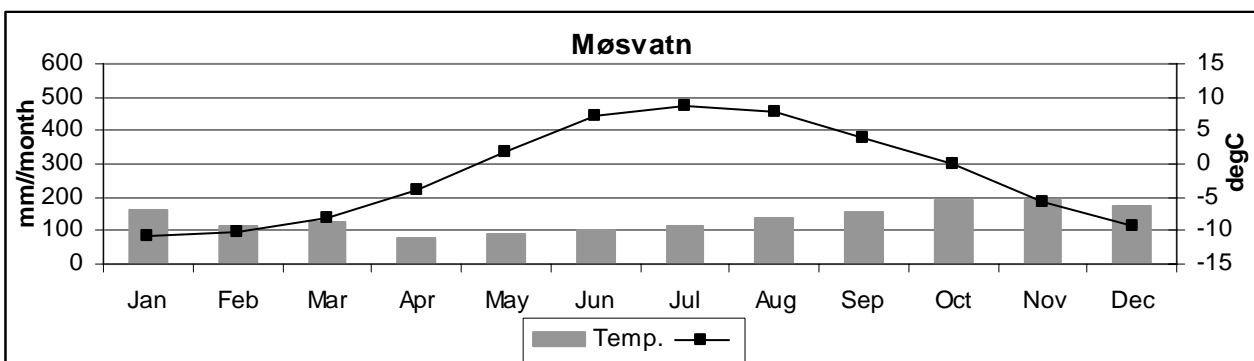


Figure 3.17 Mean monthly temperature and precipitation sum representing Møsvatn catchment. The estimates are obtained from interpolation of daily mean values estimated from observations.

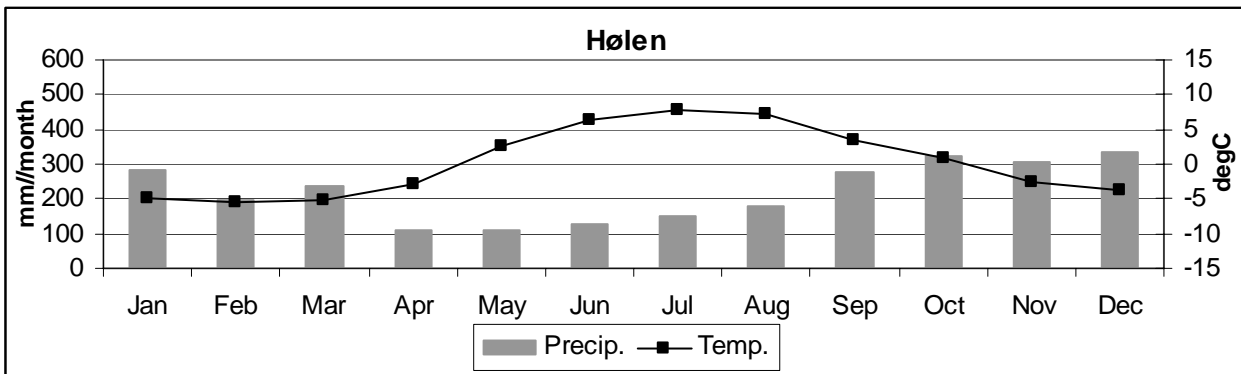


Figure 3.18 Mean monthly temperature and precipitation sum representing Hølen catchment. The estimates are obtained from interpolation of daily mean values estimated from observations.

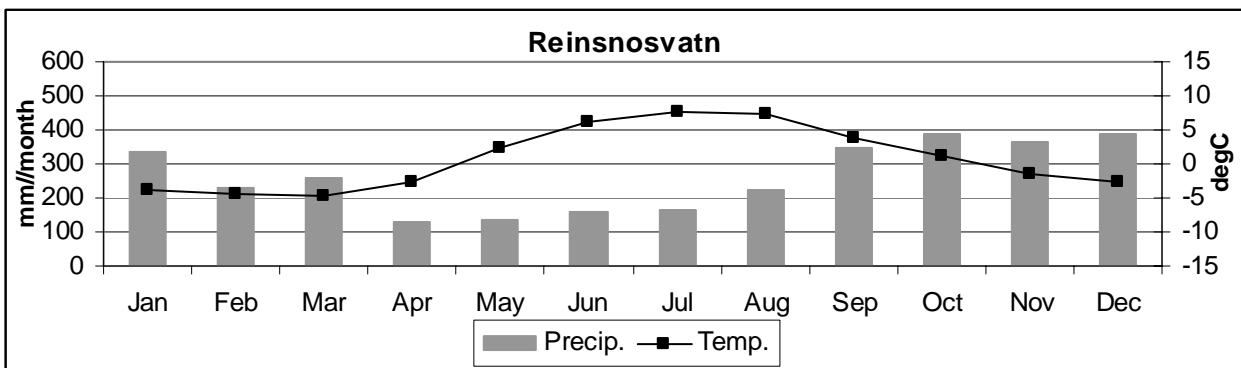


Figure 3.19 Mean monthly temperature and precipitation sum representing Reinsnosvatn catchment. The estimates are obtained from interpolation of daily mean values estimated from observations.

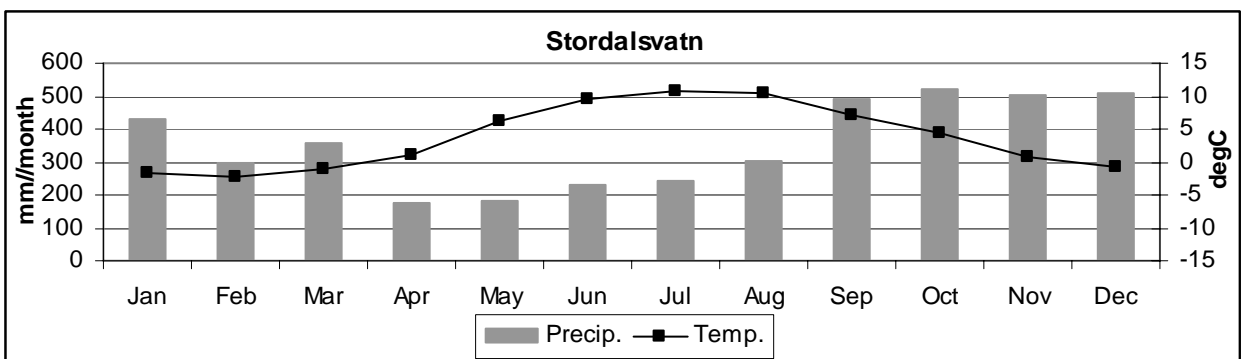


Figure 3.20 Mean monthly temperature and precipitation sum representing Stordalsvatn catchment. The estimates are obtained from interpolation of daily mean values estimated from observations.

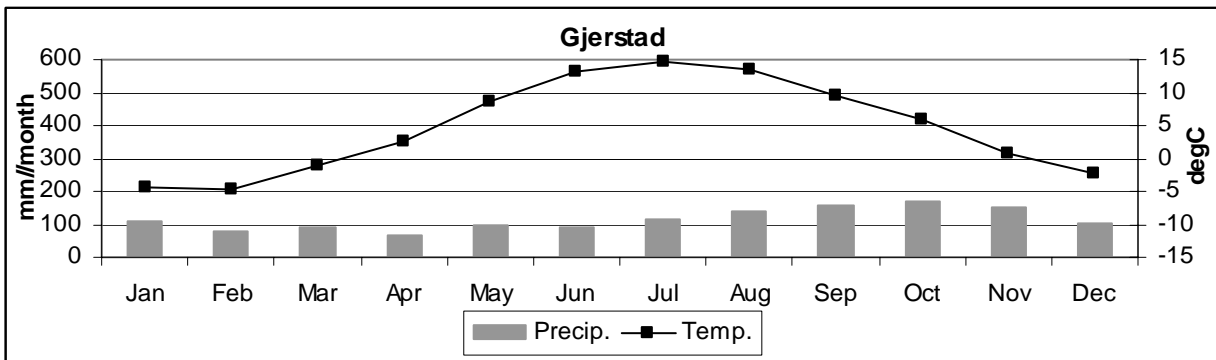


Figure 3.21 Mean monthly temperature and precipitation sum representing Gjerstad catchment. The estimates are obtained from interpolation of daily mean values estimated from observations.

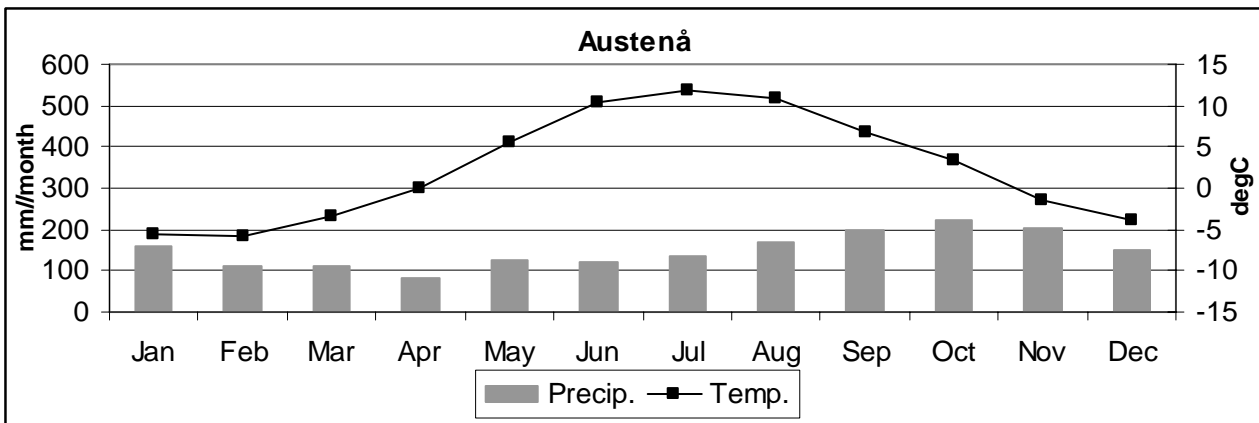


Figure 3.22 Mean monthly temperature and precipitation sum representing Austenå catchment. The estimates are obtained from interpolation of daily mean values estimated from observations.

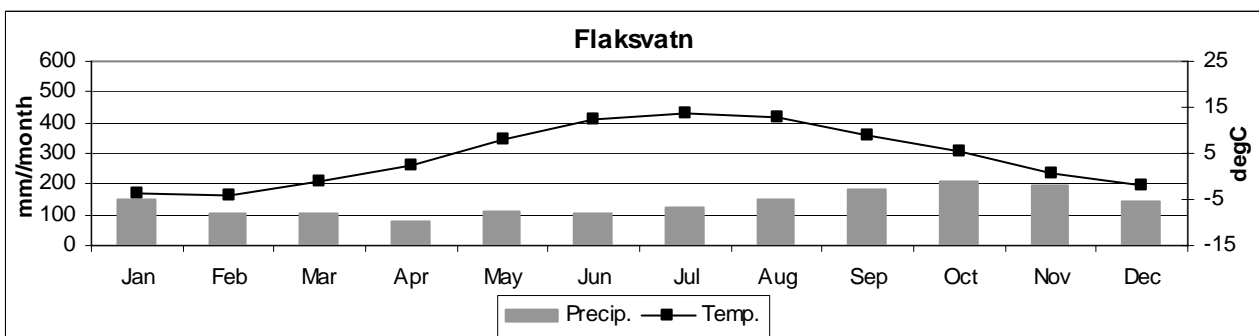


Figure 3.23 Mean monthly temperature and precipitation sum representing Flaksvatn catchment. The estimates are obtained from interpolation of daily mean values estimated from observations.

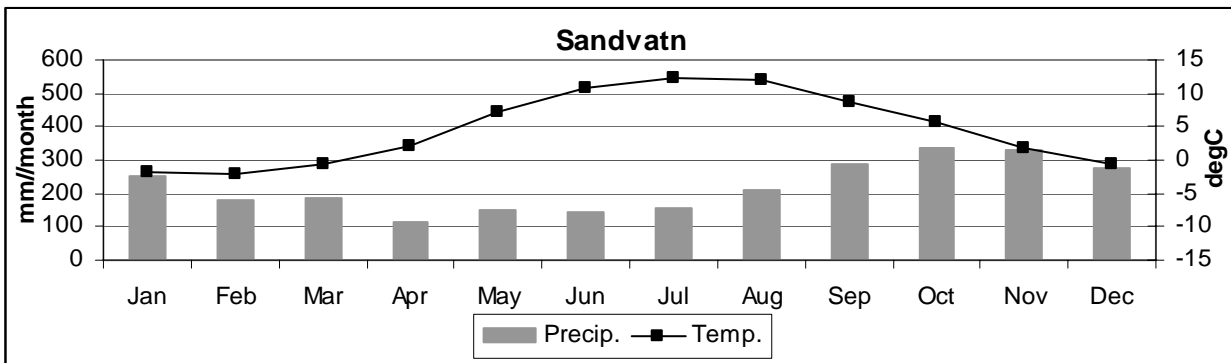


Figure 3.24 Mean monthly temperature and precipitation sum representing Sandvatn catchment. The estimates are obtained from interpolation of daily mean values estimated from observations.

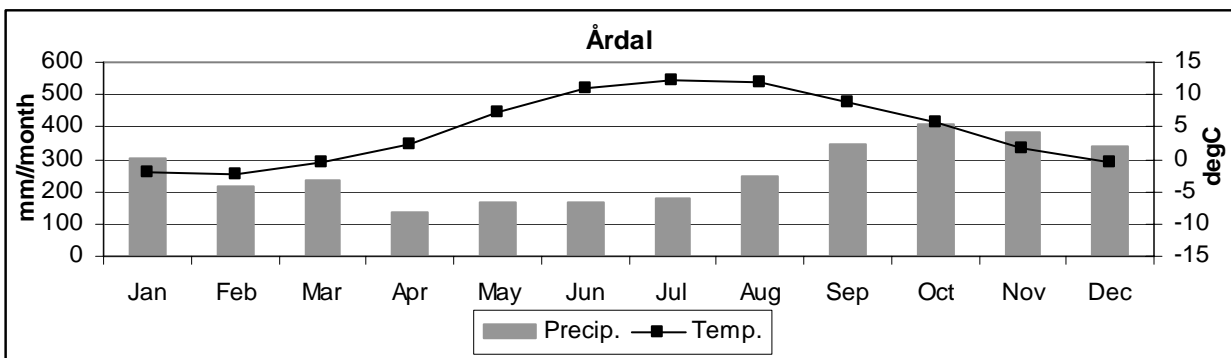


Figure 3.25 Mean monthly temperature and precipitation sum representing Årdal catchment. The estimates are obtained from interpolation of daily mean values estimated from observations.

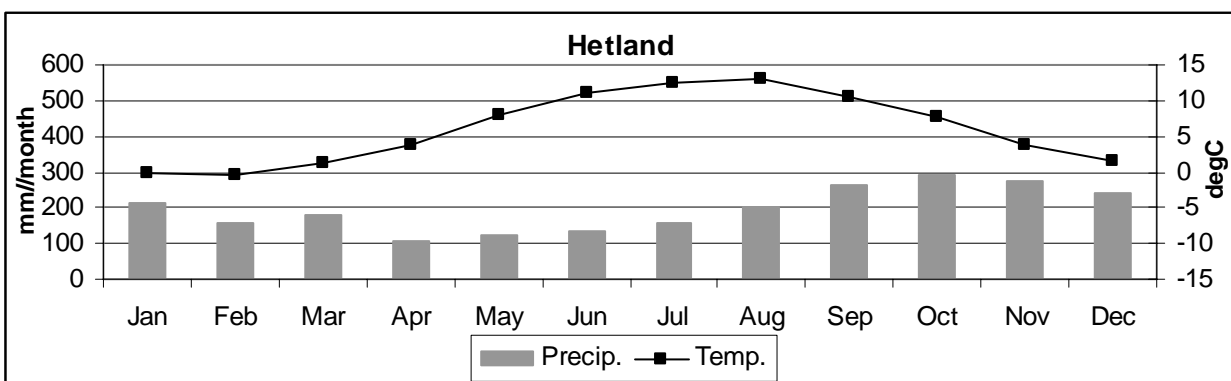


Figure 3.26 Mean monthly temperature and precipitation sum representing Hetland catchment. The estimates are obtained from interpolation of daily mean values estimated from observations.

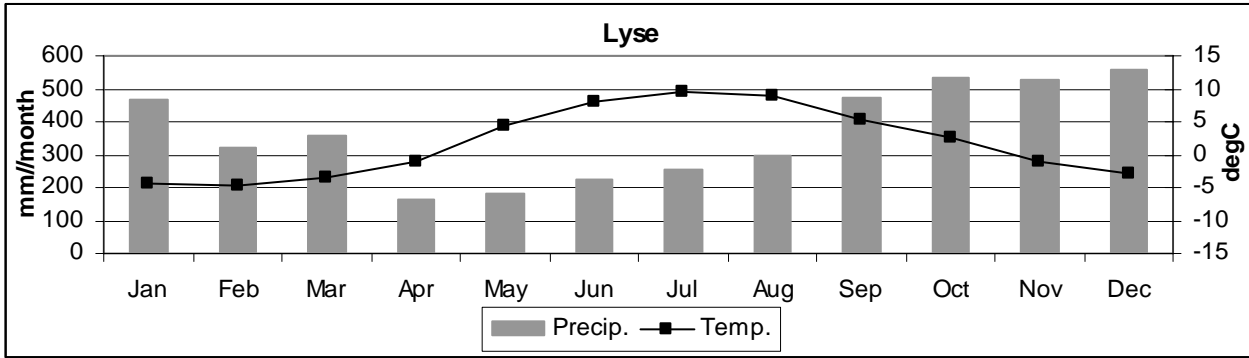


Figure 3.27 Mean monthly temperature and precipitation sum representing Lyse catchment. The estimates are obtained from interpolation of daily mean values estimated from observations.

3.2 ERA40 re-analysis

The ERA40 project is a global atmospheric analysis of many conventional observations and satellite data for the period September 1957 - August 2002 (Simmons and Gibson, 2000; Bengtsson et al. 2004). The main objective of such global analyses is to provide the best possible description of the state of the atmosphere, land and surface conditions over the period. Analyses were produced daily at 00Z, 06Z, 12Z and 18Z. The atmospheric model was run with the following resolution:

- 60 levels in the vertical;
- T159 spherical-harmonic representation for basic dynamic fields;
- a reduced Gaussian grid with approximately uniform 125 km spacing for surface and other grid-point fields.

Detailed descriptions of the project and the data assimilation system are available in The ERA-40 Project Report Series (<http://www.ecmwf.int/publications/library/do/references/list/192>) and ERA-40 Archive Plan (http://www.ecmwf.int/research/era/Products/Archive_Plan/index.html) documents from European Centre for Medium-Range Weather Forecast (ECMWF) (Uppala, et.al., 2005).

3.3 Global future climate projections

The multi-model ensemble of global climate projections made with a range of different GCMs, used here and reported in IPCC AR4 (Meehl et al., 2007), are freely available from Program for Climate Model Diagnosis and Intercomparison (PCMDI; <https://esg.llnl.gov:8443/index.jsp>). This model ensemble includes both simulations for the 20th century (c20) and scenario runs for the 21st century following the Special Report Emission Scenarios (SRES) emission scenario A1b (SRES A1b) (IPCC, 2000). Some of the GCMs have been used to make several parallel runs, differing by using different initial conditions (starting point). Table 3.1 provides an overview of the different runs downscaled in this study, a complete list of the exact runs is listed in Appendix A. The list of different runs is more complete at the PCMDI, and the ones used here is limited to the results that were available at the time of the analysis (the results were made available continuously as they were ready).

Table 3.1 Simulations from 14 different GCMs for the 20th and 21st century (A1b) (Meehl et al., 2007) is used. Empirical downscaling of temperature and precipitation are performed with temperature (101) and precipitation (601) for 68 and 67 runs respectively.

Predictor:	101	101	601	601
Emission scenario:	20th Century	sres a1b	20th Century	sres a1b
Global climate modell	No of runs	No of runs	No of runs	No of runs
BCC.cm1	2	0	0	0
BCCR.bcm2.0	1	1	1	1
CCCMA.CGCM3.1	1	1	1	1
CNRM.cm3	1	1	1	1
CSIRO.mk3.0	1	0	0	1
GFDL.cm2.0	1	1	1	1
GFDL.cm2.1	3	1	1	1
GISS.aom	1	2	2	2
GISS.modell_e.h	5	4	3	3
GISS.modell_e.r	0	0	5	2
INMCN3.0	1	1	1	1
IPSL.cm4	1	1	1	1
MIROC3.2.hires	0	1	1	0
MIROC3.2.medres	0	0	2	2
MIUB.echo.g	0	0	2	2
MPI.ECHAM5	3	3	3	2
MRI.cgcm2.3.2a	0	0	5	5
NCAR.cesm3.0	4	6	3	3
NCAR.pcm1	3	3	3	3
UKMO.hadcm3	2	2	1	1
UKMO.hadgem1	0	0	1	1

4 Empirical Statistical Downscaling (ESD) method

Mean monthly precipitation sum or mean monthly temperature (Section 3.1) was used as predictands in a ESD analysis. Gridded ERA40 precipitation or temperature over a larger region (Section 3.2) was used as predictors. The implementation was similar to the work documented in Benestad (2005, 20008a,b,c) for each GCM implemented, and performed for monthly mean values. Large-scale precipitation was used to downscale local precipitation (Benestad et al., 2007) and large-scale temperature was used to estimate local temperature. The ESD was applied to the IPCC AR4 MMD GCM ensemble (also referred to as ‘CMPI3’) for both the 20th century and the 21st century simulations separately (Section 3.3), and the tool *clim.pact* (Benestad, 2004) was used to carry out the calculations, using a common Empirical Orthogonal Function (EOF) based framework (Benestad, 2001) and linear multiple regression as a basis for the empirical-statistical model.

The common EOF framework combined large-scale gridded temperature or precipitation anomalies estimated from the ERA40 re-analysis with corresponding anomalies from a simulation performed by a GCM (interpolated onto the same grid as the former), and an ordinary EOF analysis is applied to this combined data set. The principal components (PCs) describing the temporal variations of the different

modes (predominant spatial temperature or precipitation pattern) then represent exactly the same spatial structures for GCMs and ERA40. The regression analysis uses the part of the PCs describing ERA40 together with the predictand (run-off series) to calibrate the model. This calibration returns the R^2 -statistics, describing how well the run-off can be reproduced with the statistical model if ERA40 is used as predictor (Section 4).

Because the various GCMs may differ in their ability to provide an exact representation of the spatio-temporal structure of the temperature or precipitation modes, the common EOFs may differ from GCM to GCM. Thus the R^2 -statistics may vary with the GCM, although the variation in the R^2 -statistics should be small for realistic GCMs (large deviations in the R^2 -statistics may be an indicator of model problems).

The present study is based on 14 different GCMs following the SRES emission scenario A1b. The number of simulations for the different climatic variable and time interval is shown in Appendix A, however, not all of these GCM results were used; a quality check was implemented that weeded out poorly performing models. The main criterion for being included in the ensemble was that the downscaled series displayed variability with a reasonable magnitude. For temperature, the results should not have a standard deviation outside the range of 50%-300% of observed variability, while for precipitation range for acceptable magnitude was set to 30%-300%. In addition to the quality control filter, the downscaled 20th century ('control period') series were adjusted by setting the mean value for the monthly values over the 1961-1990 interval (climatology) to equal corresponding observed 1961-1990 values. Missing values were ignored in estimating the mean monthly climatology. The downscaled SRES A1b results were then adjusted according to corresponding 20th century simulation, if available, by matching polynomial trend fits for the two segments. The SRES A1b results without a 20th century counterpart were adjusted so that they initial value corresponded to the ensemble mean value of '1999' (i.e. using the entire 20th century control ensemble). More details about the quality control filter and adjustments are given in Benestad (2008d).

The *clim.pact* tool makes predictions based on the calibration data (here ERA40) as well as the GCM (here either 20th century or the 21st century). However, the ESD-results derived from ERA40 are *not* independent and only serves as a visual check of the quality of the statistical downscaling model. The downscaling for the 20th century, on the other hand, provides independent data which can be used in the validation against the actual observations. This validation will test whether the ESD-model is good.

5 Results

Monthly precipitation sums representing twenty-five catchments in Norway are downscaled using precipitation (601) as predictor with ESD methods. The results from ~30 empirically downscaled GCMs for precipitation representing the 20th century (control runs) and the 21th century up to 2050 following SRES emission scenario A1b (IPCC, 2000) (scenario runs) are summarised in Table 5.1. The results are presented in Annex report B (Engen-Skaugen et al., 2008a). The results are summarised in Section 6.1.

Mean monthly temperature representing twenty-five catchments in Norway are downscaled using temperature (101) as predictor with ESD methods. Results from ~30 empirically downscaled GCMs for temperature representing the 20th century (control runs) and the 21st century up to 2050 following SRES emission scenario A1b (IPCC, 2000) (scenario runs) are summarised in Table 5.2. The results are presented in Annex report C (Engen-Skaugen et al., 2008b). The results are discussed in Section 6.2.

Box plot of the change in temperature and precipitation from the period 1961-1990 until 2071-2100 based on ESD of GCMs with SRES emission scenario A1b (IPCC, 2000) for the sites Oslo, Bergen, Tromsø, Trondheim (Værnes), Nesbyen (only temperature) and Gjeilo i Skjåk (only precipitation) (for location see figure 2.1) are established (see Figures 5.1 and 5.2 respectively).

Temperature and precipitation projections obtained with dynamical downscaling (within the Norwegian RegClim project) are used in e.g. Beldring et al. (2006; 2008). They used dynamically downscaled projections from the models ECHAM4/OPYC3 from the Max Plank Institute in Hamburg (Roeckner et al., 1999), with SRES emission scenario B2 (IPCC, 2000) (referred to as MPIB2) and HadAm3H from Hadley

centre, UK, with emission scenarios A2 and B2 (IPCC, 2000) (referred to as HADA2 and HADB2). The regional climate model used was HIRHAM (Bjørge et al., 2000). The climate signal obtained with these three scenarios (HADA2, HADB2 and MPIB2) for temperature (Engen-Skaugen, 2007) and precipitation are presented as dots in seasonal box plots of the projections obtained with ESD method (Figs. 5.1 and 5.2).

A description of the catchments and future projections of precipitation and temperature estimated from dynamical downscaling within the Norwegian RegClim project are given in Engen-Skaugen (2008a) and Engen-Skaugen et al. (2008b) respectively.

Table 5.1 Change in future projections for mean monthly precipitation obtained with ESD for 2021 – 2050 relative to 1961 – 1990. The error estimates represent the 90% confidence interval.

Catchments	Winter	Spring	Summer	Autumn
Masi	101 +/- 17	107 +/- 32	104 +/- 31	107 +/- 23
Kobbvatn	101 +/- 23	104 +/- 34	106 +/- 33	105 +/- 31
Nervoll	101 +/- 26	104 +/- 29	106 +/- 31	110 +/- 27
Kjelstad	100 +/- 28	102 +/- 27	104 +/- 18	105 +/- 24
Rathe	101 +/- 25	100 +/- 31	102 +/- 19	104 +/- 23
Aursunden	100 +/- 24	101 +/- 18	103 +/- 20	108 +/- 22
Nybergsund	104 +/- 29	104 +/- 36	100 +/- 28	110 +/- 36
Knappom	104 +/- 30	104 +/- 45	100 +/- 29	106 +/- 35
Risefoss	103 +/- 36	104 +/- 30	101 +/- 24	106 +/- 20
Farstad	102 +/- 28	104 +/- 41	104 +/- 27	105 +/- 24
Vistdal	104 +/- 28	103 +/- 43	103 +/- 19	105 +/- 27
Viksvatn	103 +/- 32	106 +/- 57	105 +/- 33	108 +/- 30
Sjodalsvatn	103 +/- 27	102 +/- 33	100 +/- 34	105 +/- 28
Orsjoren	103 +/- 28	104 +/- 33	98 +/- 30	107 +/- 27
Mosvatn	102 +/- 24	104 +/- 27	97 +/- 35	106 +/- 30
Holen	98 +/- 40	104 +/- 52	102 +/- 31	107 +/- 30
Reinsnosvatn	98 +/- 37	106 +/- 45	102 +/- 40	107 +/- 31
Stordalsvatn	101 +/- 38	106 +/- 46	105 +/- 33	110 +/- 34
Gjerstad	105 +/- 41	99 +/- 45	93 +/- 46	100 +/- 39
Austena	105 +/- 37	103 +/- 37	93 +/- 48	103 +/- 39
Flaksvatn	106 +/- 38	103 +/- 38	94 +/- 48	103 +/- 42
Sandvatn	102 +/- 30	106 +/- 42	96 +/- 47	107 +/- 36
Aardal	101 +/- 29	106 +/- 39	99 +/- 42	108 +/- 35
Hetland	102 +/- 22	104 +/- 34	97 +/- 35	108 +/- 30
Lyse	102 +/- 36	106 +/- 48	102 +/- 35	110 +/- 31

Table 5.2 Change in future projections for mean monthly temperature obtained with ESD from 1961 – 1990 to 2021 – 2050. The error estimates represent the 90% confidence interval.

Catchments	Winter	Spring	Summer	Autumn
Masi	3.5 +/- 4.6	2.4 +/- 2.6	1.6 +/- 1.8	2.7 +/- 2.8
Kobbvatn	1.3 +/- 2	2 +/- 2.3	1.4 +/- 1.7	2 +/- 1.8
Nervoll	3.1 +/- 4.1	1.8 +/- 2.3	1.3 +/- 1.5	2.2 +/- 2.1
Kjelstad	1.9 +/- 2.5	1.7 +/- 1.8	1.2 +/- 1.4	1.9 +/- 1.7
Rathe	1.7 +/- 2.7	1.7 +/- 1.9	1.2 +/- 1.5	1.9 +/- 1.8
Aursunden	1.7 +/- 3	1.8 +/- 2	1.3 +/- 1.4	2 +/- 1.9
Nybergsund	1.6 +/- 2.9	1.8 +/- 2	1.3 +/- 1.4	2 +/- 2
Knappom	1 +/- 2.6	1.6 +/- 1.7	1.2 +/- 1.3	1.8 +/- 1.8
Risefoss	1.7 +/- 2.2	1.7 +/- 1.7	1.2 +/- 1.2	2 +/- 1.9
Farstad	1 +/- 1.5	1 +/- 1.1	0.9 +/- 1	1.5 +/- 1.4
Vistdal	1.2 +/- 1.8	1.4 +/- 1.5	1 +/- 1.2	1.9 +/- 1.7
Viksvatn	1.2 +/- 1.5	1 +/- 1.1	1 +/- 1.2	1.4 +/- 1.4
Sjodalsvatn	1.9 +/- 2.7	1.6 +/- 1.6	1 +/- 1.3	1.8 +/- 2
Orsjoren	1.4 +/- 2.3	1.4 +/- 1.7	0.8 +/- 1.1	1.8 +/- 1.8
Mosvatn	1.1 +/- 1.9	1.4 +/- 1.6	1.2 +/- 1.4	1.7 +/- 1.8
Holen	1 +/- 1.5	1.1 +/- 1.1	0.9 +/- 1.3	1.5 +/- 1.4
Reinsnosvatn	1.1 +/- 1.4	1.1 +/- 1.1	0.9 +/- 1.2	1.5 +/- 1.4
Stordalsvatn	1.2 +/- 1.5	1.1 +/- 1.1	0.9 +/- 1.3	1.5 +/- 1.5
Gjerstad	1.3 +/- 2	1.3 +/- 1.5	1.2 +/- 1.3	1.3 +/- 1.3
Austena	1.5 +/- 2.3	1.2 +/- 1.4	1.2 +/- 1.4	1.6 +/- 1.6
Flaksvatn	1.3 +/- 1.9	1.2 +/- 1.5	1.1 +/- 1.3	1.4 +/- 1.4
Sandvatn	1.1 +/- 1.5	1.2 +/- 1.2	1.1 +/- 1.3	1.3 +/- 1.2
Aardal	1.2 +/- 1.5	1.1 +/- 1.2	1.1 +/- 1.3	1.3 +/- 1.2
Hetland	1.1 +/- 1.4	0.9 +/- 1	0.9 +/- 1.1	1.2 +/- 1.2
Lyse	1.4 +/- 1.7	1.2 +/- 1.2	1 +/- 1.3	1.5 +/- 1.5

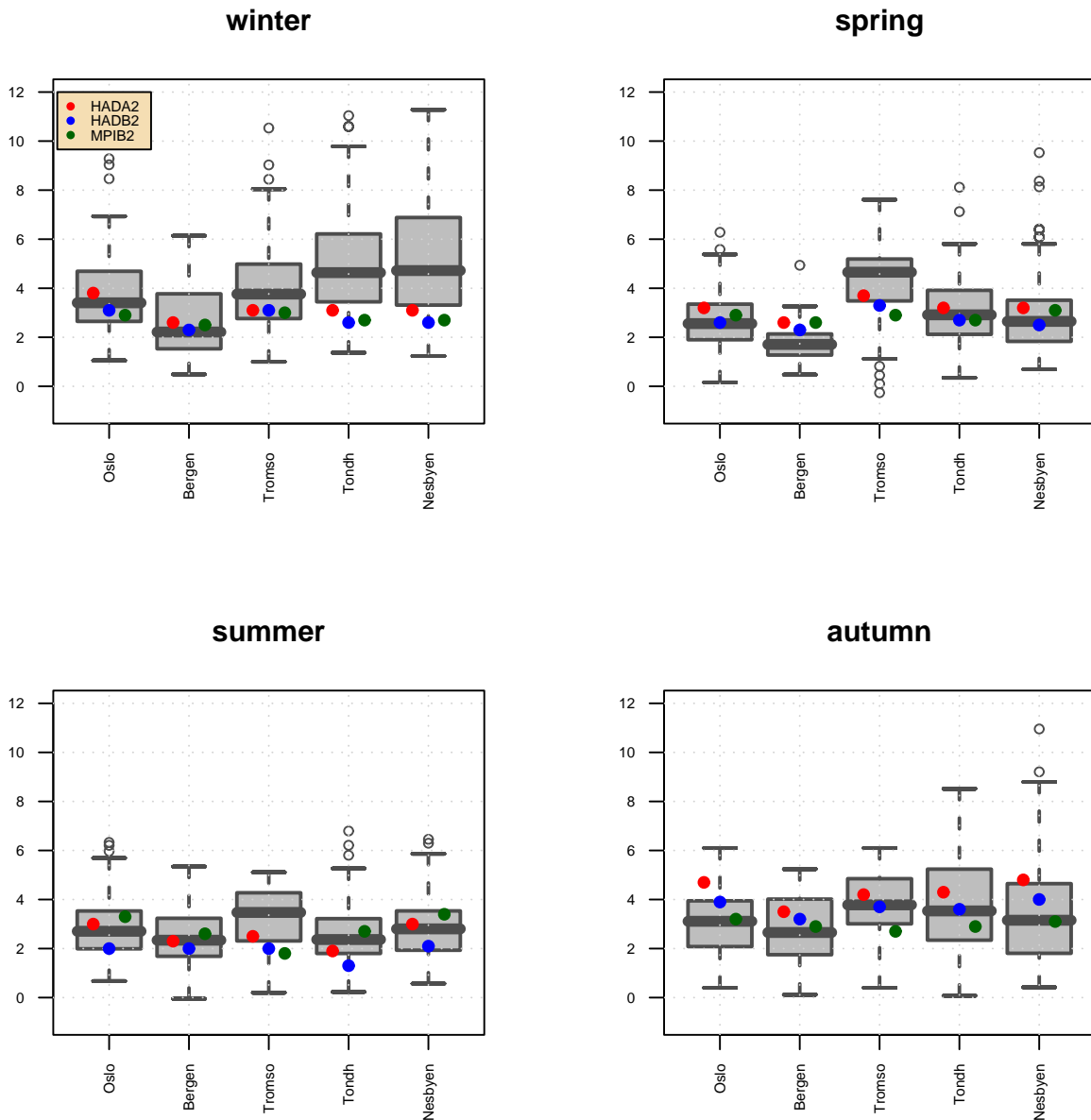


Figure 5.1 Box plots of empirically downscaled temperature for 5 locations based on multi-model IPCC AR4-based SRES A1b (CMIP3) to 5 locations in Norway (Figure 2.1). The projected change at the locations based on dynamical downscaling of the TAR-based SRES S2 and B2 emission scenarios and the GCMs ECHAM4/OPYC3 and HadAm3H is plotted in the figure; HADA2, HADB2 and MPIB2 with red, blue and green respectively. The figures show temperature change in degrees Celsius between 1961-1990 and 2071-2100.

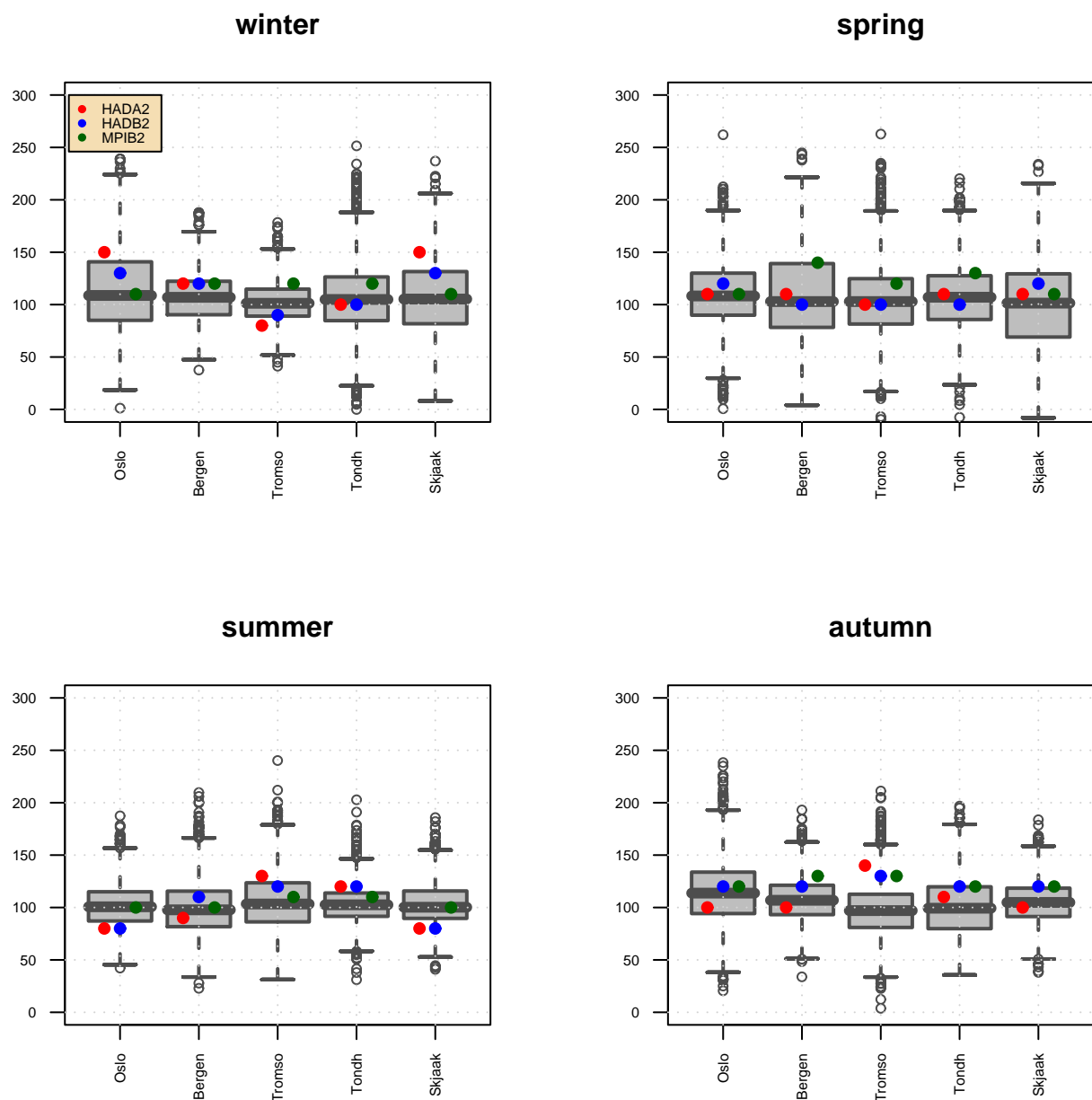


Figure 5.2 Box plots of empirically downscaled precipitation for 5 locations based on multi-model IPCC AR4-based SRES A1b (CMIP3) to 5 locations in Norway (Figure 2.1). The projected change at the locations based on dynamical downscaling of the TAR-based SRES S2 and B2 emission scenarios and the GCMs ECHAM4/OPYC3 and HadAm3H is plotted in the figure; HADA2, HADB2 and MPIB2 with red, blue and green respectively. The figures show change in precipitation in percentage between 1961-1990 and 2071-2100.

6 Discussion and concluding remarks

The present study is based on 14 different GCMs following the SRES emission scenario A1b. It is based on ~60 global model runs for the 20th and 21st century for precipitation and temperature. The time period analysed is 1960-2050 where the time period 1960 – 1990 is used as the control period. The downscaling technique used is ESD. Results on precipitation and temperature are presented in tables 5.1 and 5.2, and Engen-Skaugen et al. (2008a) and Engen-Skaugen et al. (2008b) respectively. Results on precipitation and temperature are discussed in Sections 6.1 and 6.2 respectively.

6.1 Precipitation

Figs. 2.1. - 2.25. in Appendix B (Engen-Skaugen et al., 2008a) show the empirically downscaled model runs for all the selected catchments. Gray is used for the period 1958 – 2000 and blue for the period 2000-2050. Dark shadings are used to mark the inter-quantile range (IQR; the range between the 25 and 75 percentiles) of the model results at any time, while lighter shadings are used for the range beyond these percentiles. The corresponding observed historic time series are shown as a black dotted curve in the figures, and these should therefore lie within the spread of the historical model runs if the ESD-analysis returned realistic results. The spread furthermore give an indication of the range of uncertainty of the model runs. Relative change for the future period 2000-2050 compared to the normal period 1961 – 1990 is presented in table 5.1.

The results differ somewhat to the projections obtained for the homogeneous precipitation regions presented in Benestad (2008 a). The selected catchments represent smaller regions compared to the precipitation regions and more details are contained in the historical time series leading to differences in the projections. Since the large-scale precipitation from the ERA40, used as predictor, will provide a closer match with the mean precipitation over a larger region than smaller, it is expected that the former will provide better ESD-model calibration and hence more reliable results.

A summary of the results for the selected catchments are given:

Masi, Kobbvatn and Nervoll are high mountain catchments in the northern part of Norway. Masi is largest with flat terrain located at Finnmarksvidda within precipitation region 12 (Figure 2.1). Kobbvatn and Nervoll are located in Nordland County in precipitation regions 11 and 10 respectively. Kobbvatn is the smallest catchment, but has the steepest terrain gradient.

No marked trend can be seen in the spread plots in the projections of precipitation except an increase for Nervoll in Autumn (Figs. 2.1-2.3 in Appendix B; Engen-Skaugen et al., 2008a). The figures show that the seasonal variability is captured in the projections. Table 5.1 shows that a small increase in precipitation is projected for all three catchments in spring, summer and autumn, no change is projected in Winter. The variability in winter precipitation is large. The ESD-model does not capture all of the variability for Masi by the end of the 19th century, indicating less reliable results in winter

Kjelstad, Rathe, Aursunden, Nybergsund and Knappom are located in the south-eastern part of Norway near the Swedish border. Parts of the catchments, except Kjelstad, expand into Sweden (Figure 2.1). Rathe and Kjelstad are situated in precipitation region 9, Aursunden, and parts of Nybergsund in precipitation region 7. The other part of Nybergsund and Knappom are located in precipitation region 2. **Risefoss** is located further west in high mountain regions within precipitation region 7, but close to precipitation region 8.

An increase in the projections is found in autumn for all six catchments. A positive trend in the projections is found also in summer for Kjelstad, Aursunden (Figs. 2.4-2.9 in Engen-Skaugen et al., 2008a). Table 5.1 shows that the increase is largest in autumn for all six catchments.

Farstad and Vistdal are located in the western part of the country in precipitation region 8. **Viksvatn** is situated further south in precipitation region 6 and **Sjodalsvatn** are further inland in the high mountain area in precipitation region 1, but close to precipitation regions 2 and 7 (Figure 2.1).

A positive trend can be seen in the projections in autumn until 2050 for Farstad, Vistdal, Viksvatn and Sjodalsvatn (Figs. 2.10 - 2.13 in Engen-Skaugen et al., 2008a). Minor changes are projected in winter, spring and summer. A negative trend can be seen by the end of the time period in summer for Sjodalsvatn. Mean change for the period 2021-2050 relative to 1961 – 1990 indicate an increase for all catchments and seasons, with the exception no change in Summer for Sjodalsvatn (Table 5.1).

Orsjoren, Møsvatn, Hølen, Reinsonvatn and Stordalsvatn are located in the high mountain region in southern to south-eastern Norway. Orsjoren and Møsvatn are located on the boarder between precipitation regions 2 and 6. Møsvatn are close to precipitation region 5 as well. Hølen are located to the west of

Orsjoren in precipitation region 6, Reinsnosvatn are at the boarder between precipitation region 5 and 6. Stordalsvatn are located in precipitation region 5.

Minor changes can be seen in precipitation in winter, Spring and Summer for all five catchments. Larger increase is found in autumn (Figs. 2.14.1-2.18.1 in Engen-Skaugen et al., 2008a and Table 5.1). The variability in winter precipitation is large. The ESD-model does not capture all of the variability for these catchments by the end of the 19th century, indicating less reliable results in winter (Figs. 2.14-2.18 in Engen-Skaugen et al., 2008a).

Gjerstad, Austenå, Flaksvatn, Sandvatn, Årdal, Hetland and Lyse are located in the southern part of Norway; Lyse, Hetland, Årdal and Sandvatn in the western part of the country, while Flaksvatn, Austenå and Gjerstad in the eastern side of the country. Lyse and Austenå in precipitation region 5, Hetland, Årdal and Sandvand in region 4, and Flaksvatn and Gjerstad in region 3.

Increase in winter precipitation and reduction in summer precipitation is projected Gjerstad, Austenå and Flaksvatn. Reduction in summer precipitation is projected for Sandvatn, here an increase in Spring precipitation is projected. For Årdal, Hetland and Lyse, increased spring and Autumn precipitation is projected (Figs. 2.19 – 2.25 in Engen-Skaugen et al., 2008a). The variability in winter precipitation is large. The ESD-model does not capture all of the variability for Sandvatn, Årdal, Hetland and Lyse by the end of the 19th century, indicating less reliable results in winter.

6.2 Temperature

Figs. 2.1-2.25 in Engen-Skaugen et al. (2008b) shows the empirically downscaled model runs; grey is used for the period 1958 – 2000 and blue for the period 2000-2100. Dark shadings mark the IQR, while light colours show the range of the results. Time series observed temperature are drawn as a black dotted curve in the figures, and should lie within the spread of the historical model runs. This is the case for all the selected catchments and for all seasons. The spread gives an indication of the range of uncertainty of the model runs. Relative change for the future period 2000-2050 compared to the normal period 1961 – 1990 is presented in table 6.2.

The results differ somewhat to the projections obtained for the homogeneous precipitation regions presented in Benestad (2008). The selected catchments represent smaller regions compared to the precipitation regions and more details are contained in the historical time series leading to differences in the projections.

A summary of the results are given:

Masi, Kobbvatn and Nervoll are high mountain catchments in the northern part of Norway. Masi is large with a small elevation gradient located at Finnmarksvidda within temperature region 5 (Figure 2.1). Kobbvatn and Nervoll are located in Nordland County both in temperature region 4. Kobbvatn is the smallest catchment, but has the steepest terrain gradient.

Positive trend is projected for temperature in all seasons for Masi, Kobbvatn and Nervoll. For Masi and Nervoll the trend is largest in autumn and winter. For Kobbvatn, the change is projected to be largest in autumn and spring (Figs. 2.1 - 2.3 in Engen-Skaugen et al., 2008b and Table 5.2).

Kjelstad, Rathe, Aursunden, Nybergsund and Knappom are located in the southeastern part of Norway near the Swedish border within temperature region 1. Parts of the catchments, except Kjelstad, expand into Sweden (Figure 2.1). **Risefoss** is located further west within the same temperature region, but close to temperature regions 3 and 2.

Positive trend is projected for temperature in all seasons for Kjelstad, Rathe, Aursunden, Nybergsund, Knappom and Risefoss. The projected change is largest in autumn (Figs. 2.4 – 2.9 in Engen-Skaugen et al., 2008b and Table 5.2)

Farstad, Vistdal, and Viksvatn are located in the western part of the country in temperature region 2, **Sjodalsvatn** further inland in the high mountain area on the border between temperature region 1 and 2 (Figure 2.1).

Positive trend is projected for temperature in all seasons for Farstad, Vistdal, Viksvatn and Sjudalsvatn . The projected change is largest in autumn. For Sjudalsvatn the trend is large also in winter (Figs. 2.10 – 2.13 in Engen-Skaugen et al., 2008b and Table 5.2).

Orsjoren, Møsvatn, Hølen, Reinsonvatn and Stordalsvatn are located in the high mountain region in southern to south-eastern Norway. Orsjoren and Møsvatn are located on the boarder between temperature region 1 and 2, Hølen, Stordalsvatn and Reinsnosvatn are located in temperature region 2.

Positive trend is projected for temperature in all seasons for Orsjoren, Møsvatn, Hølen, Reinsnosvatn and Stordalsvatn. The projected change is largest in autumn (Figs. 2.14 – 2.18 in Engen-Skaugen et al., 2008b and Table 5.2)

Gjerstad, Austenå, Flaksvatn, Sandvatn, Årdal, Hetland and Lyse are located in the southern part of Norway; Lyse, Hetland, Årdal and Sandvatn in the western part of the country in temperature region 2, while Flaksvatn, Austenå and Gjerstad are located in temperature region 1 in the eastern side of the country.

Positive trend is projected for temperature in all seasons for Gjerstad, Austenå, Flaksvatn, Sandvatn, Årdal and Lyse. The projected change is somewhat larger in autumn and winter (Figs. 2.19 – 2.25 in Engen-Skaugen et al., 2008b and Table 5.2).

6.3 Concluding remarks

Estimates of projected precipitation obtained with empirical statistical downscaling involve larger degree of uncertainty compared to temperature. The physical processes are more complex (thus difficult to model) and not fully understood. The model runs therefore agree less in their estimates compared to temperature. The downscaled scenarios indicate a future warming for all catchments, but the trends for precipitation are more varied.

Acknowledgement

The authors would like to thank Astrid Voksø, Norwegian Water Resources and Energy Directorate (NVE), for providing digital geographical data of the watersheds analysed.

References

- Anderson, D.L.T, and Carrington, D., 1994. Simulation of Tropical Variability as a Test of Climate Models. In: Speranza, A., and nd R. Fantechi, S.Tibaldi (eds), Global Change. Environment and Quality of Life, vol. EUR 15158 EN. European Commission.
- Beldring, S., Engen-Skaugen, T., Fjørland, E.J. and Roald, L.A., 2008, Climate change impacts on hydrological processes in Norway based on two methods for transferring regionalclimate model results to meteorological station sites, Tellus 60A, 439-450
- Beldring, S., Roald, L.A., Engen-Skaugen T., Fjørland, E.J., 2006, Climate change impacts on hydrological processes in Norway 2071 – 2100 – Based on RegClim HIRHAM and Rossby Centre RCAO Regional Climate Model Results, NVE Report no. 5 /2006 (<http://nve.no/>)
- Benestad, R.E., 2001. A comparison between two empirical downscaling strategies. Int. J. Climatology, ., 1645–1668. DOI 10.1002/joc.703.
- Benestad, R.E., 2004. Empirical-Statistical Downscaling in Climate Modeling. Eos, ,(42), p. 417.
- Benestad, R.E., 2005. Climate change scenarios for northern Europe from multi-model IPCC AR4 climate simulations. Geophys. Res. Lett., (doi:10.1029/2005GL023401), L17704.

- Benestad, R.E., Hanssen-Bauer, I., and Førland, E.J., 2007. An Evaluation of Statistical Models for Downscaling Precipitation and Their Ability to Capture Long-Term Trends. *International Journal of Climatology*, (10.1002/joc.1421), 649–665.
- Benestad, R.E. 2007 'Changes in Daily Mean, Maximum and Minimum Temperatures' met.no report 09, 2007
- Benestad, R.E., Chen, D., and Hanssen-Bauer, I., in press 2008. *Empirical-Statistical Downscaling*. Singapore: World Scientific Publishing.
- Benestad, R.E. 2008 a, Downscaled regional Norwegian temperature and precipitation series, met.no report 07/2008.
- Benestad, R.E., 2008 b, Empirical-Statistical Downscaling of Russian and Norwegian temperature series, met.no report 13/2008 Climate.
- Benestad, R.E., 2008 c, Heating degree days, Cooling degree days and precipitation in Europe. Analysis for the CELECT-project. met.no report 04/2008.
- Benestad, R.E., 2008 d, Empirical-Statistical Downscaled Arctic Temperature and Precipitation Series, met.no Report 10/08 Climate
- Bengtsson, L., 1996. The Climate response to the Changing Greenhouse Gas Concentration in the Atmosphere. In: Anderson, D.L.T., and Willebrand, J. (eds), *Decadal Variability*. NATO ASI series, vol. 44. Springer.
- Bengtsson, L., Hagemann, S., and Hodges, K.I., 2004. Can climate trends be calculated from reanalysis data? *Journal of Geophysical Research*, (doi:10.1029/2004JD004536).
- Bjørge, D., Haugen, J.E. and Nordeng, T.E., 2000, Future climate in Norway. DNMI Research Report 103, Norwegian Meteorological Institute, Oslo
- Christensen, J.H., Hewitson, B., Busuioc, A., Chen, X. Gao, Held, I., Jones, R., Kolli, R.K., Kwon, W.-T., Laprise, R., na Rueda, V. Maga Mearns, L., Menéndez, C.G., Räisänen, J., Rinke, A., Sarr, A., and Whetton, P., 2007. *Climate Change: The Physical Science Basis*. United Kingdom and New York, NY, USA: Cambridge University Press. Chap. 11 Regional Climate Projections.
- Crane, R.G., and Hewitson, B.C., 1998. Doubled CO₂ Precipitation Changes for the Susquehanna Basin: Downscaling from the Genesis General Circulation Model. *International Journal of Climatology*, , 65–76.
- Engen-Skaugen, T., Benestad, R.E., and Roald, L.A., 2007. Empirically downscaling of runoff in Norway; Is it feasible? *Climate* 15. met.no, <http://met.no>.
- Engen-Skaugen, T., Benestad, R.E., and Førland, E.J., 2008a. Resultd from ESD analyses on precipitation representing twenty-five Norwegian catchments. met.no report no 23 b/08, <http://met.no>.
- Engen-Skaugen, T., Benestad, R.E., and Førland, E.J., 2008b. Resultd from ESD analyses on temperature representing twenty-five Norwegian catchments. met.no report no 23 c/08, <http://met.no>.
- Hanssen-Bauer, I., and Førland, E.J., 1998. Annual and seasonal precipitation variations in Norway 1896-1997. *Klima* 27/98. DNMI.
- Hanssen-Bauer, I., and Nordli, P.Ø., 1998. Annual and seasonal temperature variations in Norway 1896-1997. *Klima* 25/98. DNMI. .
- Houghton, J.T., Ding, Y., Griggs, D.J., Noguer, M., van der Linden, P.J., Dai, X., Maskell, K., and Johnson, C.A., 2001. *Climate Change 2001: The Scientific Basis*. Contribution of Working Group I to the Third Assessment Report of IPCC. International Panel on Climate Change, (Available from www.ipcc.ch).
- IPCC (2000) Special report on emission scenarios. A special report of working group III of the intergovernmental Panel on Climate Change. In: Nakicenovic N, Alcamo J, Davis G, de Vries B, Fenham J, Gaffin S, Gregory K, Gru'bler A, Young Jung T, Kram T, La Rover EL, Michaelis L, Mori S, Morita T,

Pepper W, Pitcher H, Price L, Rihai K, Roehrl A, Rogner HH, Sankovski A, Schlesinger M, Shukla P, Smith S, Swart R, van Rooijen S, Victor N, Dadi Z (eds)]. Cambridge University Press, Cambridge IPCC, 1995. The Second Assessment Report. Technical Summary. WMO and UNEP, [http://www.ipcc.ch/pub/sa\(E\).pdf](http://www.ipcc.ch/pub/sa(E).pdf).

Jansson, A., Tveito, O.E., Pirinen, P. and Scharling, M., 2007, NORDGRID – a preliminary investigation on the potential for creation of a joint Nordic gridded climate dataset, met.no report No. 03/2007

Meehls, G.A., Stocker, T.F., W.D. Idlingstein, Gaye, A.T., Gregory, J.M., Kitoh, A., Knutti, R., Murphy, J.M., Noda, A., Raper, S.C.B., Watterson, I.G., Weaver, A.J., and Zhao, Z.-C., 2007. Climate Change: The Physical Science Basis. United Kingdom and New York, NY, USA: Cambridge University Press. Chap. Global Climate Projections. Nakicenovic, N, J, Alcamo, G, Davis, de Vries B, J, Fenhann, S, Gaffin, K, Gregory, A, Grubler, T, Young Jung, T, Kram, EL, La Rover, L, Michaelis, Mori S, Morita T, W, Pepper, H, Pitcher, L, Price, K, Rihai, A, Roehrl, HH, Rogner, A, Sankovski, M, Schlesinger, P, Shukla, S, Smith, R, Swart, van Rooijen S, N, Victor, and Z, Dadi (eds)., 2000. Special report on emission scenarios. A special report of working group III of the intergovernmental Panel on Climate Change. Cambridge University Press, Cambridge. Chap. 4.

Philander, S.G., 1989. El Niño, La Niña, and the Southern Oscillation. N.Y.: Academic Press.

Robinson, P.J., and Finkelstein, P.L., 1991. The development of impact-oriented scenarios. Bull. Am. Met. Soc., , 481–490.

Roeckner E., Bengtsson, L., Feichter, J., Leliveld, J., Rodhe H., 1999, Transient climate change simulations with a coupled atmosphere-ocean GCM including the tropospheric sulphur cycle. J. Clim. 12, 3004-3032.

Sarachik, E.S., Winton, M., and Yin, F.L., 1996. Mechanisms for Decadal-to-Centennial Climate Variability. In: Anderson, D.L.T., and Willebrand, J. (eds), Decadal Variability. NATO ASI series, vol. 44. Springer.

Simmons, A. J., and Gibson, J. K., 2000. The ERA-40 Project Plan. ERA-40 Project Report Series. ECMWF.

Solomon, S., Quin, D., Manning, M., Chen, Z., Marquis, M., Averyt, K.B., Tignotr, M., and Miller, H.L. (eds)., 2007. Climate Change: The Physical Science Basis. Contribution of Working Group I to the Fourth Assessment Report of the Intergovernmental Panel on Climate Change. United Kingdom and New York, NY, USA: Cambridge University Press.

Treut, H. Le., 1994. Cloud Representation in Large-Scale Models: Can we Adequately Constrain them through Observed Data? In: Speranza, A., and nd R. Fantechi, S. Tibaldi (eds), Global Change. Environment and Quality of Life, vol. EUR 15158 EN. European Commission.

Tveito, O.E., Wegehenkel, M. van der Wel, F., Dobesch, H., 2008, EUR 23461 – COST Action 719 – Earth System Science and Environmental Management – The Use of Geographic Information Systems in Climatology and Meteorology (246 pp).

Tveito, O.E., 2007, The development in spatialisation of meteorological and climatological elements, pp 73-86 in H. Dobesch, P. Dumolard and I. Dyras (eds): Spatial interpolation for climate data, ISTE books, London, UK, 284pp

Tveito, O. E.; Bjørndal, I., Skjelvåg, A.O. and Aune, B. (2005) A GIS-based agro-ecological decision system based on gridded climatology, *Meteorological Applications*, 12:1:57-68

Uppala, S.M., Kållberg, P.W., Simmons, A.J., Andrae, U., da Costa Bechtold, V., Fiorino, M., Gibson, J.K., Haseler, J., Hernandez, A., Kelly, G.A., Li, X., Onogi, K., Saarinen, S., Sokka, N., Allan, R.P., Andersson, E., Arpe, K., Balmaseda, M.A., Beljaars, A.C.M., van de Berg, L., Bidlot, J., Bormann, N., Caires, S., Chevallier, F., Dethof, A., Dragosavac, M., Fisher, M., Fuentes, M., Hagemann, S., Hólm, E., Hoskins, B.J., Isaksen, L., Janssen, P.A.E.M., Jenne, R., McNally, A.P., Mahfouf, J.-F., Morcrette, J.-J., Rayner, N.A., Saunders, R.W., Simon, P., Sterl, A., Trenberth, K.E., Untch, A., Vasiljevic, D., Viterbo, P.,

and Woollen, J. 2005: The ERA-40 re-analysis. *Quart. J. R. Meteorol. Soc.*, 131, 2961-3012.doi:10.1256/qj.04.176

von Storch, H., Zorita, E., and Cubasch, U., 1993b. Downscaling of Global Climate Change Estimates to Regional Scales: An Application to Iberian Rainfall in Wintertime. *Journal of Climate*, , 1161–1171.

Wilby, R.L., Charles, S.P., Zortia, E., Timbal, B., Whetton, P., and Mearns, L.O., 2004. Guidelines for Use of Climate Scenarios Developed from Statistical Downscaling Methods. Supporting material of the Intergovernmental Panel on Climate Change. Task group on Data and Scenario Support for Impacts and Climate Analysis.

Zorita, E., and von Storch, H., 1997. A survey of statistical downscaling results. Tech. rept. 97/E/20. GKSS.

Appendix A

A complete list showing which global climate model runs that is used in the analyses. C20 means 20th century, sresa1b means 20th century following the SRES emission scenario A1b. 101 and 601 are predictors used, daily mean temperature [°C] and daily precipitation sums [mm/day] respectively.

GCM	Period	101	601
BCC.cm1	c20	run1	run1
BCC.cm1	c20	run2	run2
BCCR.bcm2.0	c20	run1	run1
BCCR.bcm2.0	sresa1b	run1	run1
CCCMA.CGCM3.1	c20	run1	run1
CCCMA.CGCM3.1	sresa1b	run1	run1
CNRM.cm3	c20	run1	run1
CNRM.cm3	sresa1b	run1	run1
CSIRO.mk3.0	c20	run1	run1
CSIRO.mk3.0	sresa1b		run1
GFDL.cm2.0	c20	run1	run1
GFDL.cm2.0	sresa1b	run1	run1
GFDL.cm2.1	c20	run1	run1
GFDL.cm2.1	c20	run2	run2
GFDL.cm2.1	c20	run3	run3
GFDL.cm2.1	sresa1b	run1	run1
GISS.aom	c20	run2	run2
GISS.aom	c20		run1
GISS.aom	sresa1b	run1	run1
GISS.aom	sresa1b	run2	run2
GISS.modell_e.h	c20	run1	run1
GISS.modell_e.h	c20	run2	
GISS.modell_e.h	c20	run3	run3
GISS.modell_e.h	c20	run4	run4
GISS.modell_e.h	c20	run5	run5
GISS.modell_e.h	sresa1b	run1	run1
GISS.modell_e.h	sresa1b	run2	run2
GISS.modell_e.h	sresa1b	run3	run3
GISS.modell_e.r	sresa1b	run1	
GISS.modell_e.r	sresa1b	run2	run2
GISS.modell_e.r	sresa1b	run3	
GISS.modell_e.r	sresa1b	run4	run4
GISS.modell_e.r	sresa1b	run5	
INMCN3.0	c20	run1	run1
INMCN3.0	sresa1b	run1	run1
IPSL.cm4	c20	run1	run1

IPSL.cm4	sresa1b	run1	run1
MIROC3.2.hires	c20		run1
MIROC3.2.hires	sresa1b	run1	
MIROC3.2.medres	sresa1b	run2	run2
MIROC3.2.medres	sresa1b	run3	run3
MIUB.echo.g	sresa1b	run1	run1
MIUB.echo.g	sresa1b	run3	run3
MPI.ECHAM5	c20	run1	run1
MPI.ECHAM5	c20	run2	run2
MPI.ECHAM5	c20	run3	run3
MPI.ECHAM5	sresa1b	run1	run1
MPI.ECHAM5	sresa1b	run2	
MPI.ECHAM5	sresa1b	run3	run3
MRI.cgcm2.3.2a	sresa1b	run1	run1
MRI.cgcm2.3.2a	sresa1b	run2	run2
MRI.cgcm2.3.2a	sresa1b	run3	run3
MRI.cgcm2.3.2a	sresa1b	run4	run4
MRI.cgcm2.3.2a	sresa1b	run5	run5
NCAR.cesm3.0	c20	run1	run1
NCAR.cesm3.0	c20	run3	run3
NCAR.cesm3.0	c20		run5
NCAR.cesm3.0	c20	run6	run6
NCAR.cesm3.0	c20		run7
NCAR.cesm3.0	c20	run9	run9
NCAR.cesm3.0	sresa1b	run1	run1
NCAR.cesm3.0	sresa1b	run2	run2
NCAR.cesm3.0	sresa1b	run3	run3
NCAR.pcm1	c20	run2	run2
NCAR.pcm1	c20	run3	run3
NCAR.pcm1	c20	run4	run4
NCAR.pcm1	sresa1b	run1	run1
NCAR.pcm1	sresa1b	run2	run2
NCAR.pcm1	sresa1b	run3	run3
UKMO.hadcm3	c20	run1	run1
UKMO.hadcm3	c20	run2	run2
UKMO.hadcm3	sresa1b	run1	run1
UKMO.hadgem1	sresa1b	run1	run1